Clim Dyn (2008) 31:79–105
DOI 10.1007/s00382-007-0340-z

Projected changes in drought occurrence under future global warming from multi-model, multi-scenario, IPCC AR4 simulations

Justin Sheffield · Eric F. Wood

Received: 24 July 2007 / Accepted: 5 November 2007 / Published online: 27 November 2007

Abstract Recent and potential future increases in global temperatures are likely to be associated with impacts on the hydrologic cycle, including changes to precipitation and increases in extreme events such as droughts. We analyze changes in drought occurrence using soil moisture data for the SRES B1, A1B and A2 future climate scenarios relative to the PICNTRL pre-industrial control and 20C3M twentieth century simulations from eight AOGCMs that participated in the IPCC AR4. Comparison with observation forced land surface model estimates indicates that the models do reasonably well at replicating our best estimates of twentieth century, large scale drought occurrence, although the frequency of long-term (more than 12-month duration) droughts are over-estimated. Under the future projections, the models show decreases in soil moisture globally for all scenarios with a corresponding doubling of the spatial extent of severe soil moisture deficits and frequency of short-term (4–6-month duration) droughts from the mid-twentieth century to the end of the twenty-first. Long-term droughts become three times more common. Regionally, the Mediterranean, west African, central Asian and central American regions show large increases most notably for long-term frequencies as do mid-latitude North American regions but with larger variation between scenarios. In general, changes under the higher emission scenarios, A1B and A2 are the greatest, and despite following a reduced emissions pathway relative to the present day, the B1 scenario shows smaller but still substantial increases in drought, globally and for most regions. Increases in drought are driven primarily by reductions in precipitation with increased evaporation from higher temperatures modulating the changes. In some regions, increases in precipitation are offset by increased evaporation. Although the predicted future changes in drought occurrence are essentially monotonic increasing globally and in many regions, they are generally not statistically different from contemporary climate (as estimated from the 1961–1990 period of the 20C3M simulations) or natural variability (as estimated from the PICNTRL simulations) for multiple decades, in contrast to primary climate variables, such as global mean surface air temperature and precipitation. On the other hand, changes in annual and seasonal means of terrestrial hydrologic variables, such as evaporation and soil moisture, are essentially undetectable within the twenty-first century. Changes in the extremes of climate and their hydrological impacts may therefore be more detectable than changes in their means.

J. Sheffield (✉) · E. F. Wood
Department of Civil and Environmental Engineering,
Princeton University, Princeton, NJ 08544, USA
e-mail: justin@princeton.edu

1 Introduction

The climate varies naturally in response to external forcings, such as solar radiation (Christensen and Lassen 1991) and atmospheric aerosols (Robock and Mao 1995), and because of internal interactions between components of the climate system (Trenberth and Hurrell 1994). The extremes of these variations have consequences on the terrestrial water cycle that impact human activities in terms of changes to the availability or absence of water, e.g., flooding or drought (Higgins et al. 2000; Dai et al. 1998). When coupled with potential climate change, which may impact regionally and exaggerate the influence of natural variability, the extremes of climate may become more pronounced (Easterling et al. 2000; Palmer and Räisänen 2002). To design and implement

strategies to minimize climate change or mitigate against the detrimental impacts (Hasselmann et al. 2003), it is essential to be able to detect whether climate change is actually occurring and to what extent. This is problematic because the climate change signal may be small relative to the natural variability of the climate system (Hulme et al. 1999) and may thus be undetectable, at least over the short term. The possibility then arises that by the time the signal becomes detectable, adverse impacts may have already occurred and it may be too late to reverse the change or even adapt to it (Pittock 1999; King 2004).

Climate change is often measured by changes in primary climate variables such as global surface air temperature and precipitation. These variables are first order drivers of climate impacts, inducing changes in weather extremes, sea ice thinning and glacier retreat, and thus are appropriate for studying the broader issues in climate change. They are also the best-observed variables over large scales with relatively long historical records. Recent changes in climate may be large enough to be detectable now, although this will depend on the climate variable and our level of confidence in detecting change (Hegerl et al. 2006). Analysis of the instrumental record indicates that recent increases in global annual temperature are anomalous and more rapid compared to the long-term record (e.g., Jones et al. 1999; Hansen et al. 1999; Brohan et al. 2006) and model results suggest that this cannot be due to natural variability alone (Jansen et al. 2007). However, changes in global variables may bear little relation to regional changes, especially for precipitation (Giorgi and Bi 2005) and thus changes in, for example, droughts and floods that may have serious impacts on human and environmental welfare.

The potential acceleration of the hydrologic cycle under recent and future global warming is of considerable interest (Huntington 2006), especially in terms of changes in regional variability and extremes. Of all natural disasters, the economic and environmental consequences of drought are among the highest, due primarily to the longevity and widespread spatial extent of many droughts (Wilhite 2000). Thus the potential impacts of climate change on drought are most pertinent. As temperatures rise, the capacity of the atmosphere to hold moisture would increase as governed by the Clausius–Clapeyron equation (Held and Soden 2000), with potential for increased evaporation and/or precipitation (Trenberth 1999), although these may be limited by other factors such as available energy and aerosol concentration. Climate model studies have shown that variability is likely to increase under plausible future climate scenarios (Wetherald and Manabe 2002), dependent upon climate sensitivity, with large regional changes in the water cycle. The potential for more droughts and of greater severity is a worrisome possibility (Gregory et al. 1997; Wetherald and Manabe 1999; Wang 2005), compounded by positive feedbacks, such as increases in the frequency of heat waves (Seneviratne et al. 2006a, b) and decreased carbon uptake by vegetation (Ciais et al. 2005).

Several studies using climate models have suggested that the interior of the northern hemisphere continents will become drier over the next century, especially in the summer (Rind et al 1990; Gregory et al. 1997; Wetherald and Manabe 1995, 1999, 2002). Gregory et al. (1997) analyzed summer drought over southern Europe and central North America in terms of precipitation and soil moisture from a single integration of the Hadley climate model forced by 1% year^{-1} increasing CO_2 concentrations. They found increases in multivariate drought statistics that were driven primarily by evaporation through increased temperatures but also decreased precipitation in the form of fewer events. Wetherald and Manabe (1999) analyzed soil moisture from the GFDL climate model for three scenarios: increasing greenhouse gases, increasing sulphate–aerosol and combination of both. They similarly found summer dryness and winter wetness in North America and southern Europe as well as other semi-arid regions, although high latitudes showed increasing wetness. Based on a threshold of one standard deviation, changes in soil moisture did not become detectable for several decades. In summarizing such studies, the third Intergovernmental Panel on Climate Change (IPCC) report (IPCC 2001) concluded that increased drought risk over these regions was "likely".

More recently, Giorgi (2006) analyzed a set of IPCC 4th Assessment Report (AR4) simulations and calculated a climate change index based on changes in precipitation and temperatures means and variability. He found major climate change "hot-spots" in the Mediterranean and Northern Europe, followed by high northern latitudes and Central America. Other hot-spots occur in Southern Equatorial Africa, the Sahara and eastern North America. Wang (2005) analyzed a large set of IPCC AR4 models in terms of consensus changes in precipitation, temperature and soil moisture and found inter-model consistency in some regions of northern mid- and high-latitudes in predicting summer dryness and winter wetness. In terms of drought, Burke et al. (2006) calculated the Palmer Drought Severity Index (PDSI), a commonly used drought index, from the latest version for the Hadley centre climate model for the SRES A2 scenario and found regionally strong wetting and drying, but a net global drying trend resulting in an increase in the area of extreme drought from 1 to 30% by end of this century. The conclusion of the latest IPCC report (IPCC 2007, Chap. 10, p. 783) was that "In a warmer future climate, most Atmosphere–Ocean General Circulation Models project increased summer dryness and winter wetness in most parts of the northern middle and high latitudes. Summer dryness indicates a greater risk of drought."

The consensus from these and other studies into the hydrologic impacts of future warming and the synthesis conclusions of the past two IPCC reports point towards a greater risk of drought during the twenty-first century. In this paper we investigate how drought is expected to change in the future by analyzing soil moisture and drought characteristics over global land areas, excluding Antarctica, from a suite of climate model simulations carried out under the auspices of the IPCC AR4. We quantify the change in global and regional drought occurrence relative to both the present day and the pre-industrial era, as represented by twentieth century and pre-industrial control simulations, respectively. We take into account the uncertainty in regional climate change by using data from multiple climate models and for three future climate scenarios that represent a range of plausible emission pathways.

Although global warming is expected to accelerate the hydrologic cycle and thus the occurrence and severity of drought, the changes may not become detectable for several decades (Wetherald and Manabe 1999). The detectability of climate change can be quantified by how long we have to monitor for to detect significant changes against the background of natural variability, which is basically a signal to noise problem (McCabe and Wolock 1997; Zheng and Basher 1999; Ziegler et al. 2003). The greater the variability, the harder it is to detect a signal. We use this concept to evaluate the detectability of potential future changes by applying statistical analyzes to time series of drought occurrence to determine when and where changes will become detectable. Detectability is a function of the natural variability of the system, the magnitude of the change we are interested in and the level of risk we are prepared to accept in statistical testing, among others factors, and we carry out a set of sensitivity experiments to evaluate their impact.

This study is the first that we are aware of that analyzes potential changes in drought under future global warming, as characterized by persistence in severe soil moisture deficits, from multiple models and scenarios. Previous studies have assessed predicted changes in mean climate and specifically soil moisture (Wetherald and Manabe 2002; Wang 2005) that will likely (but not necessarily) induce changes in drought. Here, we take into consideration changes in the full distribution of pertinent variables and not just the mean or some other tendency measure. Furthermore, we analyze actual model output as opposed to derived products such as the PDSI that may suffer from inadequacies, which will enhance uncertainty in the results. In terms of models and scenarios analyzed, previous studies have focused on single models and/or single scenarios (e.g., Wetherald and Manabe 2002; Wang 2005; Burke et al. 2006). To instil confidence in the robustness of assessment of future change, it must take into account the uncertainty in future climates because of model differences as well as the diversity of possible emission pathways as represented by the different scenarios. Nevertheless, uncertainties are inherent in this study, such as biases induced by the specific models and approaches we take and we highlight these where relevant.

The paper is laid out as follows. After presenting the datasets and methods we briefly evaluate how well the models represent drought during the twentieth century against off-line estimates. This is critical to our confidence in the models to project future changes. We then show how drought is expected to change over the twenty-first century for the three future climate scenarios, globally and regionally, and where these changes are statistically significant relative to contemporary climate variability as derived from twentieth century simulations. Mechanisms for the expected changes are presented next, that show how changes in evaporation, as forced by increasing temperatures, modify the primary impacts of precipitation changes and how this can be altered by changes in snow at higher latitudes. In Sect. 4 we investigate the detectability of these changes and how this depends on the time period, drought characteristic, level of significance and background variability against which the change is quantified. This section also looks at how drought detectability compares to that for other hydro-climatic variables and whether we are likely to detect changes in extremes, such as drought, earlier than changes in the mean of primary climate variables, such as annual precipitation.

2 Datasets and methods

2.1 Climate model simulations

To estimate potential future climate change we use data from the IPCC AR4 General Circulation Model (GCM) simulations. The range of future climates predicted by GCMs is large and regionally dependent (NRC 2003; Giorgi and Bi 2005) and we therefore use data from multiple GCMs and three scenarios: the Special Report on Emissions Scenarios (SRES) A2, A1B and B1 (Nakićenović et al. 2000). Each scenario represents different mixes of changes in population, economic output, land use, and energy and technology use, among others, but can be generally characterized by maximum atmospheric CO_2 concentrations. B1 represents relatively slow population growth and an emphasis on environmental protection, with CO_2 concentrations stabilized at 550 ppm by the end of the century. A1B describes a future of very rapid economic growth, global population that peaks in mid-century and declines thereafter, and the rapid introduction of new and more efficient technologies with a balance between fossil and non-fossil energy sources and is characterized by maximum concentrations of 720 ppm. A2 describes a

Table 1 Models used in this study, which have monthly soil moisture data available for the PICNTRL, 20C3M and SRES B1, A1B and A2 scenarios

Model name	Modeling group	Country
CGCM3.1(T47)	Canadian Centre for Climate Modelling & Analysis	Canada
GFDL-CM2.1	US Department of Commerce/NOAA / Geophysical Fluid Dynamics Laboratory	USA
GISS-ER	NASA/Goddard Institute for Space Studies	USA
INM-CM3.0	Institute for Numerical Mathematics	Russia
IPSL-CM4	Institut Pierre Simon Laplace	France
MIROC3.2(medres)	Center for Climate System Research (The University of Tokyo), National Institute for Environmental Studies, and Frontier Research Center for Global Change (JAMSTEC)	Japan
MRI-CGCM2.3.2	Meteorological Research Institute	Japan
ECHAM5/MPI-OM	Max Planck Institute for Meteorology	Germany

heterogeneous world with continuously increasing global population and regionally orientated economic development and fragmented technological change and is generally regarded as a worst-case scenario that sees a four to five-fold increase in CO_2 emissions over 2000–2099 during which CO_2 concentrations increase from about 350 to 850 ppm. We also use data from the corresponding pre-industrial control (PICNTRL) and twentieth century simulations (20C3M), which were also run in coupled mode, i.e., with a free-running ocean component. The 20C3M simulations are driven by prescribed historical greenhouse gas concentrations, sulphate-aerosol loadings and other forcings since the start of the industrial revolution. We use data for eight models (Table 1) which were selected as those which had soil moisture and ancillary data available for all these scenarios. Where ensemble simulations for a particular scenario were available we use the first ensemble member but it should be noted that single simulations were available more often than not.

2.2 Drought estimation

We define drought occurrence as an extended period of anomalously low soil moisture. The amount of water in the soil provides a useful indicator of drought as it reflects the aggregate effect of all hydrologic processes from changes in short-term precipitation events and temperature swings to long-term changes in climate, and can represent the status of agriculture and potential hydrologic recharge to rivers and reservoirs (Sheffield et al. 2004). Empirical probability distributions are derived for the modelled soil moisture fields for each month from the pre-industrial control simulations and the current state of drought is characterized by the quantile of the current soil moisture value in relation to the control period distribution. A drought is defined as a consecutive sequence of months of length D with soil moisture quantile values, $q(\theta)$, less than a chosen threshold, $q_0(\theta)$. Here we use a value of 10%, which reflects conditions that occur only once every 10 years for a particular month on average and so reflects rare events, and has been shown to be applicable to identifying historic events at global scales (Sheffield and Wood 2007). We are particularly interested in how individual dry months are organized into sequences of consecutive dry months that can then be considered a drought with associated deleterious impacts. Drought can be characterized in various ways and we define a number of statistics based on duration (D), intensity (I), severity (S) and areal extent (A) that are also dependent on q_0 (θ):

$$I = \frac{1}{D}\sum_{t=t_1}^{t+D-1} q_0(\theta) - q(\theta)_t \tag{1}$$

$$S = I \times D \tag{2}$$

Intensity is the mean magnitude over the duration of the drought and severity is the time integrated deficit below the threshold, with units of (% months). For example, a drought that lasted for 10 months and had a mean deficit below the threshold (intensity) of 7% would have a severity of 70% months. We also define three classes of drought depending on their duration: short-term (4–6 months), medium term (7–12 months), and long-term (longer than 12 months), although we only show results for short- and long-term droughts.

$$D_{4-6}, \text{ short-term:} \quad 4 \le D \le 6, \quad q(\theta) <= q_0(\theta) \tag{3}$$

$$D_{7-12}, \text{ medium-term:} \quad 7 \le D \le 12, \quad q(\theta) <= q_0(\theta) \tag{4}$$

$$D_{12+}, \text{ long-term:} \quad D > 12, \quad q(\theta) <= q_0(\theta) \tag{5}$$

The spatial extent of drought, A, is defined as follows:

$$A = \frac{\sum_{i=1}^{N} A(i) = \{q(\theta) <= q_0(\theta)\}}{\sum_{i=1}^{N} A(i)} \tag{6}$$

where $A(i)$ is the area of grid cell i weighted by the cosine of the grid cell latitude and N is the total number of grid cells in the region of interest.

2.3 Statistical methods

Changes in the occurrence of drought are calculated between the PICNTRL and 20C3M and future climate simulations, although we focus mainly on changes relative to the 20C3M data. The pre-industrial PICNTRL simulations are used to represent natural variability; the 20C3M simulations are used to represent present day drought conditions under contemporary climate. Changes are estimated for the ensemble of climate models to take into account the uncertainty due to model differences. We also investigate changes for a single model in Sect. 4.5 using multiple ensemble members from the same model, where uncertainty in the representation of climate is based on intra-ensemble differences rather than inter-model differences. In both cases, for each model or ensemble member, we calculated the frequency of drought and other statistics in 30-year periods. For the 20C3M simulation this was done for the period 1961–1990, assuming this to be representative of contemporary climate. For the future climate simulations we calculated statistics over a 30-year moving window. For the PICNTRL simulation, statistics were calculated for each non-overlapping, consecutive 30-year period. To account for the differences in the PICNTRL simulation length among models, which would bias the results of the multi-model assessment towards a model with a longer simulation, we simply averaged the values in each 30-year period over the whole simulation for each model.

Changes in drought are identified by testing the null hypothesis that the distribution of a drought statistic across all models has the same mean as the distribution across all models during a future time period. Student's t test statistic, which is a measure of the ratio of the difference in means to the combined variance of the two distributions, is calculated at each grid cell and the null hypothesis is rejected for t-test values greater than the critical value at confidence level α (usually taken as 0.05 or 95%). In this case we conclude that a statistically significant change has occurred. Application of the test assumes that the means of the two samples do not deviate substantially from a normal distribution.

2.4 Data preparation

We focus on monthly values for all calculations, which is the smallest time scale for which data are available for the complete period of each simulation from the IPCC database. Monthly values of soil moisture for each model are available as depths of water and are normalized to volumetric values by dividing by the field capacity, which is given for each model as a fixed field. This ensures that the soil moisture data for each model are analyzed with respect to their dynamic range as governed by soil characteristics and meteorological conditions, and are thus inter-comparable. The volumetric data are then interpolated from each model's native grid to a 2.0-deg regular grid, which is a representative scale across the set of models. Ancillary variables (e.g., precipitation) that are used in subsequent analysis of drought forcing are interpolated in the same manner.

3 Results

First, we evaluate the representation of drought in the climate models by considering (1) the natural occurrence of drought as derived from the control simulations and (2) drought under contemporary climate from the twentieth century simulations. In Sect. 3.2 we compare the twentieth century results with observation-based data to determine whether the models are capable of reproducing our best estimates of large-scale contemporary drought occurrence. Sections 3.3–3.5 present the projected future changes in drought, their statistical significance relative to contemporary climate (as estimated from 1961 to 1990 of the 20C3M data) and natural variability (as estimated from the PICNTRL data), and the driving mechanisms of change.

3.1 Natural variability of drought from GCM control simulations

Figure 1 shows the global distribution of drought statistics in terms of the multi-model ensemble mean. The statistics are the frequency of $D_{4–6}$ and D_{12+} droughts, the mean drought duration, D_{mean}, and the mean drought severity, S_{mean}. For each model, the drought statistics are calculated over 30-year blocks within the control period and then the mean is calculated over all blocks. The maps in Fig. 1 show the multi-model mean and standard deviation (inter-model variability) of the individual model means.

For $D_{4–6}$ droughts, the highest frequencies are located in mid-latitudes and the Tropics, with peak values of about 1–2 droughts per 30 years in the Pacific northwest and eastern United States, central Europe and Asia, China and central Africa. Low frequencies (<0.5 droughts 30 year^{-1}) occur in arid regions where soil moisture is persistently low and does not change much from year to year, and in high latitudes where freezing temperatures and snow cover

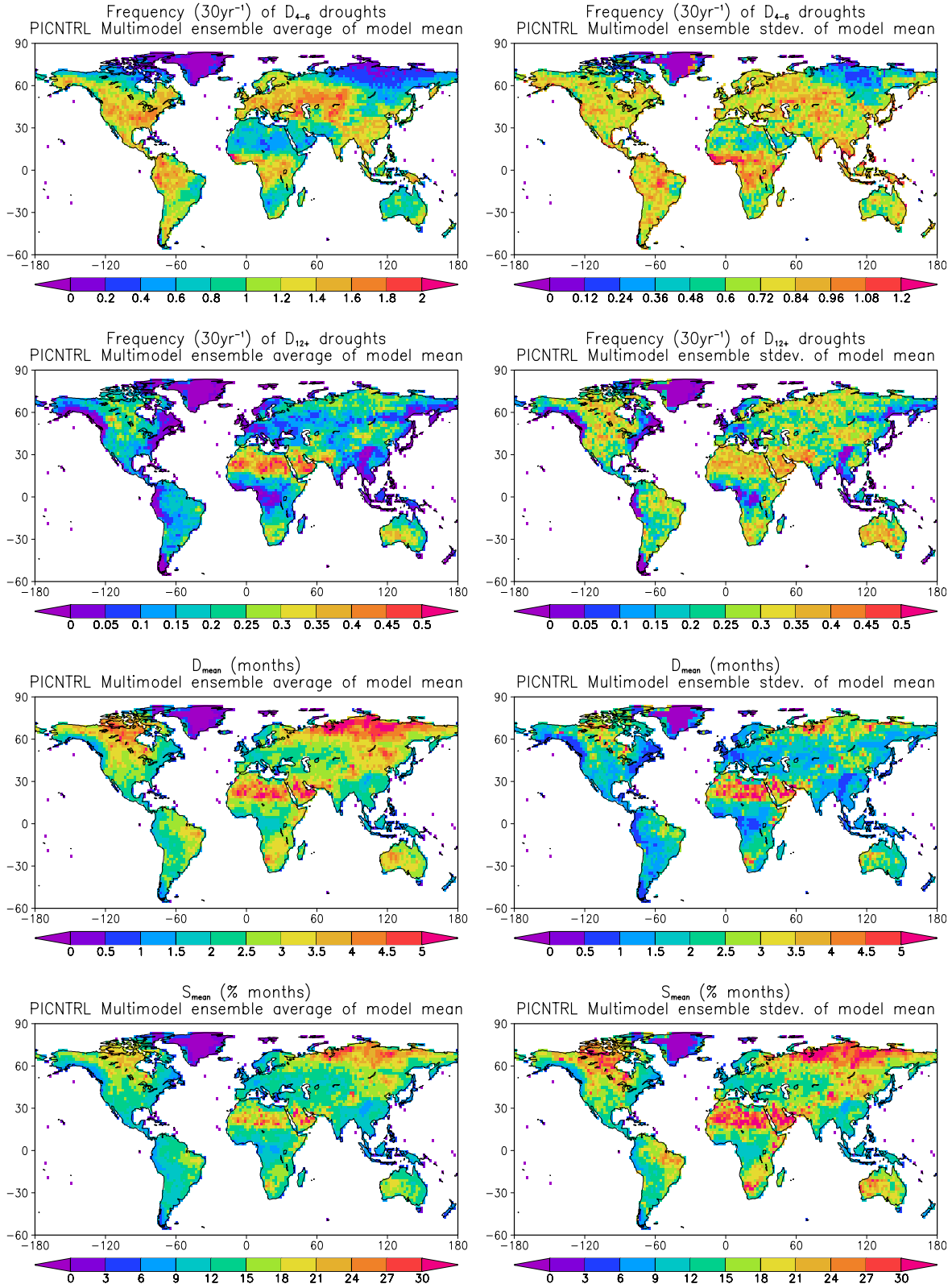

Fig. 1 Multimodel ensemble drought statistics for the pre-industrial control (PICNTRL) simulation. The statistics are number of 4–6-month duration droughts (30 yearr^{-1}), number of 12+-month duration droughts (30 year^{-1}), mean drought duration (months) and mean drought severity (% months). The statistics are calculated for 30-year periods within the each models control period and then averaged all 30 year periods. The multimodel ensemble mean and standard deviation are shown on the *left and right hand side*, respectively

prolong soil moisture anomalies (Wang 2005; Sheffield and Wood 2007). The standard deviation or inter-model variability is largest in regions of high seasonality, such as the edges of the footprint of the Inter Tropical Convergence Zone (ITCZ) in Africa and lowest in dry regions and high latitudes.

The distribution of D_{12+} frequencies is generally the opposite of that for short-term droughts, with maxima in central and northern North America, eastern south America, Siberia, and eastern Asia among others. High values are also prevalent in dry regions although as the range in soil moisture is so small, the absolute magnitude of drought is also very small. Minima are mostly located in regions with more seasonally uniform climates such as central tropical Africa, parts of southeast Asia and the eastern and Pacific northwest coasts of North America. The standard deviation values are also at a maximum in high latitudes and globally are relatively high compared with the mean, possibly indicating a lack of consensus across models in how drought varies on longer time scales. Mean drought duration and severity are similarly distributed being that severity is dominated by drought duration at low threshold values. Mean drought duration is at a maximum in high latitudes, central North America, Brazil, southern Africa and Australia.

3.2 Twentieth century drought and comparison with off-line modeling

Comparison of soil moisture data from the IPCC AR4 20C3M simulations with field measurements have been carried out by Li et al. (2007) over small regions in the Northern Hemisphere based on the database of Robock et al. (2000). They found that the models simulated the seasonal cycles for Ukraine, Russia, and Illinois adequately, but were generally poor for Mongolia and China. Importantly, all models failed to replicate observed summer drying in Russia and the Ukraine during the latter part of the twentieth century. Here we are interested in the large-scale, long-term statistics of drought as characterized by persistent soil moisture deficits. A comparison of global and regional averaged drought characteristics from the 20C3M simulations with observation-based estimates is shown in Fig. 2. The regions are shown in Fig. 3 and are defined by Giorgi and Francisco (2000) with the inclusion of the northeast Canada region (NEC) in place of the Canadian-Greenland (GRL) region. We also define the WORLD region as continental land areas excluding Greenland and Antarctica. The observation-based statistics are derived from off-line simulations using the Variable Infiltration Capacity (VIC) land surface model (Sheffield and Wood 2007), forced by an observation-based

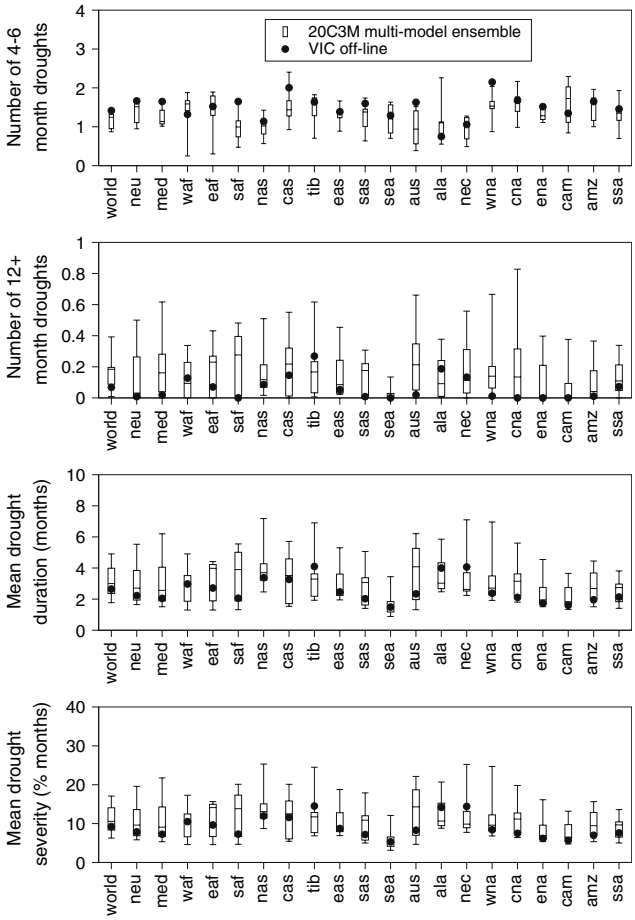

Fig. 2 Regionally averaged $D_{4–6}$ and D_{12+} frequencies, D_{mean} and S_{mean} for 1961–1990 from the twentieth century (20C3M) simulations (*box and whispers*) and an observation forced land surface model simulation (*black dots*). The *box and whispers* represent the inter-quartile range and the range (maximum and minimum values) of the set of GCMs

meteorological dataset (Sheffield et al. 2006). Because of the lack of large scale, long-term monitoring of soil moisture, observation forced off-line modeling provides the best possible estimate of historic soil moisture values at continental to global scales (Maurer et al. 2002; Sheffield et al. 2006, Guo and Dirmeyer 2006).

The climate model values in Fig. 2 generally encapsulate observation-based values, although the spread among models and the occurrence of outliers can be large depending on the region and statistic (e.g., CAM for $D_{4–6}$, SAF for D_{12+}, AUS for D_{mean}). For D_{mean} and S_{mean}, the agreement is reasonably good and the observation-based values fall within the maximum and minimum range for nearly all regions and generally lie within the inter-quartile range of the model distribution. This is consistent with Seneviratne et al. (2006a, b) who, as part of the Global Land Atmosphere Coupling Experiment (GLACE), showed that AGCMS were capable of distinguishing between observed regions of high and low soil moisture memory on

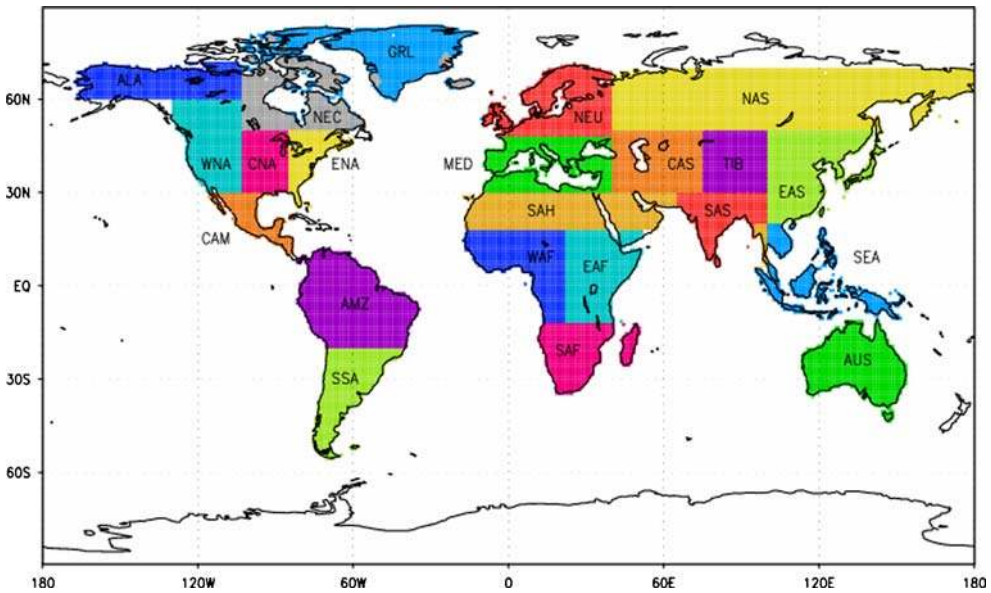

Fig. 3 Map of regions used in the analysis as defined by Giorgi and Francisco (2000). The original GRL region is split into northeastern Canada (*NEC*) and Greenland for this study

monthly time scales. For the most part, the climate model values tend to be higher, most notably for D_{12+} frequencies, D_{mean} and S_{mean}, although for the former this is a result, in part, of the zero lower bound in most regions. The general overestimation by the models of long-term drought frequencies and mean drought duration points to an underestimation of climate variability that has been noted previously (e.g., Collins et al. 2002; Hunt 2006).

3.3 Global and regional drought under future climate scenarios

Next we investigate how soil moisture and drought are predicted to change under future climates. Global averaged time series of monthly mean soil moisture and drought characteristics for the three future climate scenarios are shown in Fig. 4. For these models, the future climate simulations were initialized from the end of the 20C3M simulation and we prepend these data (in terms of the multi-model distribution) to the future scenario time series. Globally, soil moisture decreases under all scenarios, with corresponding increases in drought spatial extent. Note that the spatial extent of drought may not be contiguous which is more likely for larger regions. Corresponding changes in drought statistics (frequency of D_{4-6} and D_{12+} droughts and S_{mean}) are all increasing. In general, the increases in drought statistics are greatest under the higher emissions scenario, A2, and least under the lower emissions scenario, B1 (Table 2). The global spatial extent of drought across all models roughly doubles by 2070–2099 under all scenarios relative to the PICNTRL and 20C3M scenarios. The frequency of D_{4-6} droughts also doubles and D_{12+} droughts become two and three times more frequent relative to the PICNTRL and 20C3M scenarios, respectively. The spread in model projections as quantified by the inter-quartile range (IQR) is, however, fairly large, even at the beginning of the twenty-first century (also noted previously in the twentieth century comparisons in Sect. 3.2) and this increases by the end of the century, such that the lower bound on projections shows little change over the century, although these are invariably increases.

Figures 5, 6 and 7 show the multi-model mean, regionally averaged time series of D_{4-6} and D_{12+} frequencies and A. Similar to the global results, most regions show increases in drought statistics, but with large variation between regions and across scenarios. In particular, the MED, WAF, CAS and CAM regions show large increases, most notably for D_{12+} frequencies. The mid-latitude North American regions (WNA, CNA, ENA) also show increases but with larger variation between scenarios. Changes over high latitudes (ALA, NEC, NEU, NAS), eastern mid-latitude Asia (EAS, TIB) and regions bordering the Indian Ocean (EAF, SAS, SEA) are relatively small. The frequency of D_{12+} droughts actually decreases in NEU. Again, changes under the B1 scenario are the least and the A1B and A2 results are similar.

3.4 Statistical significance of changes

We next evaluated the statistical significance of changes in drought by the end of the twenty-first century with respect

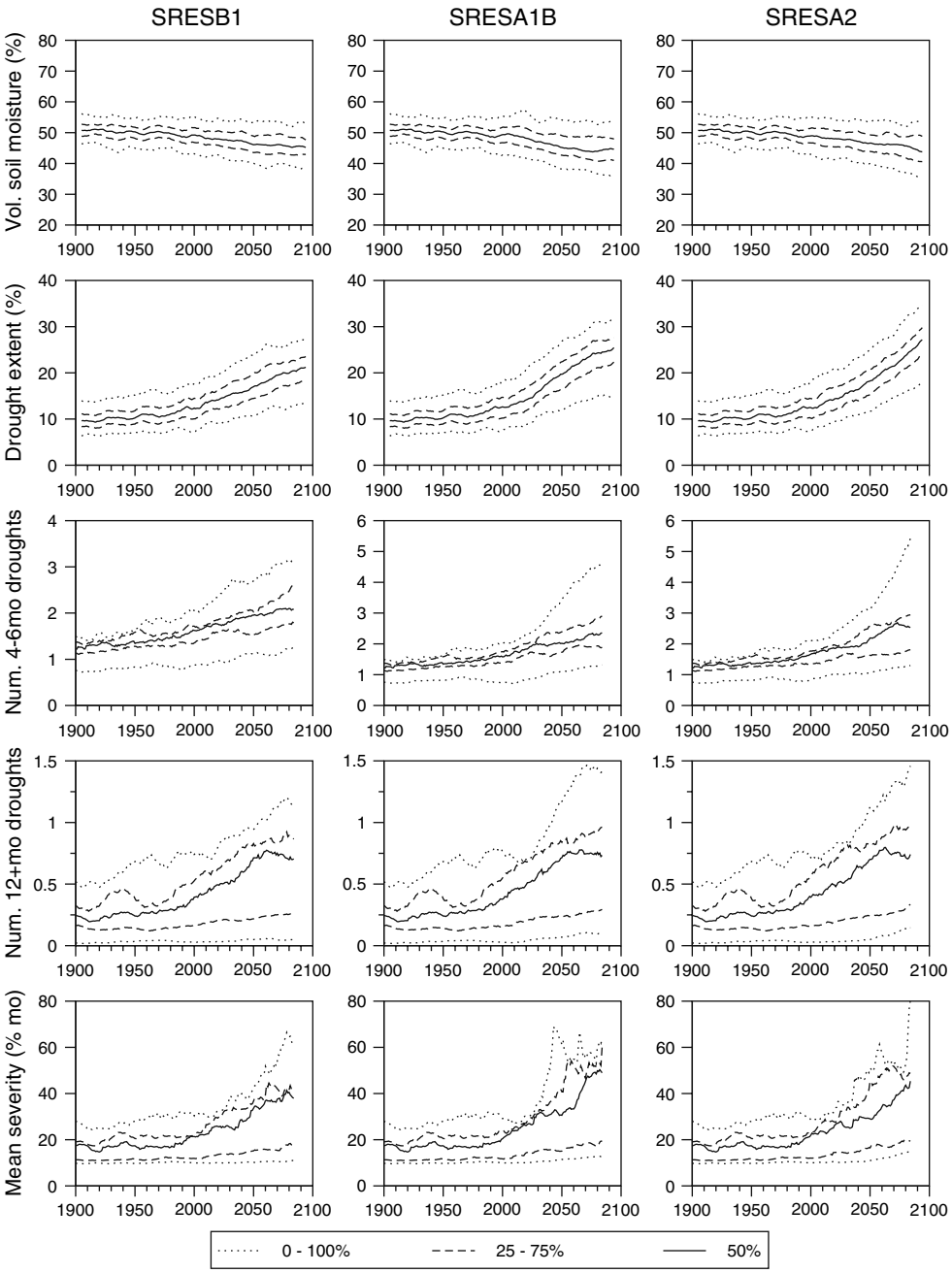

Fig. 4 Global average time series of soil moisture and various drought statistics for the twenty-first century for the SRESB1, SRESA1B and SRESA2 scenarios. Monthly soil moisture and drought extent ($q_0(\theta) = 10.0\%$) is shown as the 121-month running mean. The frequency of 4–6 month duration droughts ($q_0(\theta) = 10.0\%$), 12+-month duration droughts ($q_0(\theta) = 50.0\%$) and the maximum severity (defined as the drought intensity times the drought duration) are calculated over a 30-year moving window. The data are shown as the 0, 25, 50, 75 and 100% percentiles of the distribution of the multimodel ensemble of soil moisture and drought statistics

to the twentieth century as represented by the 1961–1990 period of the model 20C3M simulation (Figs. 8, 9). In general, D_{4-6} drought frequency increases globally between the twentieth century and the future period (Fig. 8). Large areas experience greater than 5 short-term droughts per 30 years (averaged over all models) that are statistically significant at the 95% level, including southern Europe, large parts of the USA, the Amazon, southern South America, central west Africa and scattered regions in Asia. Statistically significant changes in D_{12+} drought frequency are less spatially extensive (Fig. 9), with both increases and decreases scattered across the globe. The small extent of decreases is mostly restricted to high latitudes and generally results in zero frequencies. Increases in the southern US, Central America, the Mediterranean and southern Africa, are of the order of 2 droughts 30 year^{-1}. The spatial distribution of changes is fairly robust across scenarios, but with magnitudes greatest under the A2 scenario, and lowest under B1. Figure 10 and Table 3 summarize the regionally averaged D_{4-6} and D_{12+} drought frequencies and spatial extent of drought for the PICNTRL and 20C3m (1961–1990) simulations and the projected changes and their statistical significance for the three future climate scenarios (2070–2099). Note that increases in D_{4-6} drought frequency

Table 2 Summary of multi-model global mean soil moisture and drought characteristics for the PICNTRL, 20C3M and future climate SRES B1, A1B and A2 scenarios

	PICNTRL	20C3M (1961–1990)	SRES B1 (2070–2099)	SRES A1B (2070–2099)	SRES A2 (2070–2099)
SM (%)	50.8, 0.9	49.8, 4.0	45.8, 5.6	44.7, 7.4	44.9, 7.3
A (%)	9.2, 1.0	11.2, 3.1	18.9, 6.2	22.3, 7.2	23.0, 6.7
D_{4-6} (30 year^{-1})	1.1, 0.3	1.4, 0.3	2.2, 0.8	2.6, 1.0	2.8, 1.1
D_{12+} (30 year^{-1})	0.2, 0.14	0.3, 0.2	0.6, 0.6	0.7, 0.7	0.7, 0.6
D_{mean} (months)	3.0, 1.4	3.2, 1.7	4.7, 3.3	5.4, 4.9	5.2, 3.6
S_{mean} (months %)	14.8, 7.0	17.8, 9.3	31.9, 22.2	39.8, 40.7	38.2, 29.3

The first of each pair of values is the multi-model mean and the second is the multi-model IQR. The individual model PICNTRL values are calculated as the average of the values in each 30-yr period within the whole simulation period, whose length varies among models and is between 330 and 500 years

are statistically significant for about half the regions and scenarios and for most regions for spatial extent. Significant changes in D_{12+} frequencies are restricted to the MED, and CNA regions for all scenarios and the WORLD, SAF, CAM and SSA regions for the higher emission scenarios only. In particular the MED region shows more than 2, 3 and 3 times increase in D_{4-6} and D_{12+} drought frequency and A, respectively since 1961–1990.

3.5 Drivers of changes in drought occurrence

Figure 11 shows how predicted changes in regional drought are skewed towards the warm season. The figure shows the multi-model mean of regional averaged, monthly frequency of occurrence of soil moisture deficits for $q_0(\theta) < 10.0\%$ for the PICNTRL, 20C3M and the three future climate scenarios. By definition the PICNTRL frequencies are 10% for all months. The 20C3M and SRES frequencies are progressively larger, with 20C3M < B1 < A1B < A2 as noted previously. Warm season increases are nearly always greater than those in cooler seasons. For southern hemisphere regions, such as SAF, AMZ, SSA and AUS, the largest changes are predominantly in the austral spring. In cooler regions (NAS, ALA, NEC), increased frequencies tend to be concentrated in the warm season and increases in the cool season, especially for ALA and NAS, are minimal.

Precipitation and temperature are the primary drivers of drought. Increases in temperature will potentially increase transpiration and direct evaporation from the soil through increased atmospheric demand, while increases in precipitation will tend to increase soil moisture. Conversely, decreases in temperature and precipitation will tend to increase and decrease soil moisture respectively. However the contribution of future changes in temperature and precipitation to changes in drought occurrence under future climates is not straightforward because of the complex interactions between these forcing variables and hydrologic processes at the earth's surface. This is complicated further by changes in mean precipitation versus changes in precipitation frequency and intensity and the seasonality of changes, especially in snow dominated regions. Apart from precipitation, the key linkage between climate change and changes in soil moisture is evaporation. Although temperature increases will tend to increase potential evaporation, actual evaporation may be enhanced or diminished by precipitation increases and decreases respectively.

Model projections of future climates show increases in temperature globally and for all regions whereas changes in precipitation are regionally and often scenario dependent as shown for three example regions in Fig. 12. These regions were chosen as they show diversity in changes in future drought. The MED region shows some of the largest increases in drought frequency that is robust across models (Sect. 3.3). This can be directly attributed to reductions in precipitation totals, especially in the warm season, accompanied by reductions in runoff and soil moisture (Fig. 12). Changes in evaporation are limited to small decreases in the summer, driven by reduced precipitation that is not offset by increased atmospheric demand from higher temperatures in an already water limited environment. In the CNA region, drought occurrence is expected to increase but changes in other variables are mixed. Precipitation is expected to increase in the spring but decrease in the summer. Coupled with increased temperature, this leads to increased evaporation in the spring but little change in the summer as decreased precipitation likely outweighs any increases in potential evaporation.

Changes in drought in the NAS region are modest but are focused on the summertime and are generally representative of other high latitude regions. The hydrology in these regions is dominated by snow and ice processes which, given increases in air temperature in these regions, can explain the seasonally disproportionate changes in soil moisture deficits. Warmer temperatures tend to reduce the snow cover through melting of the existing pack and increasing the ratio of rainfall to snowfall. Precipitation is also predicted to increase

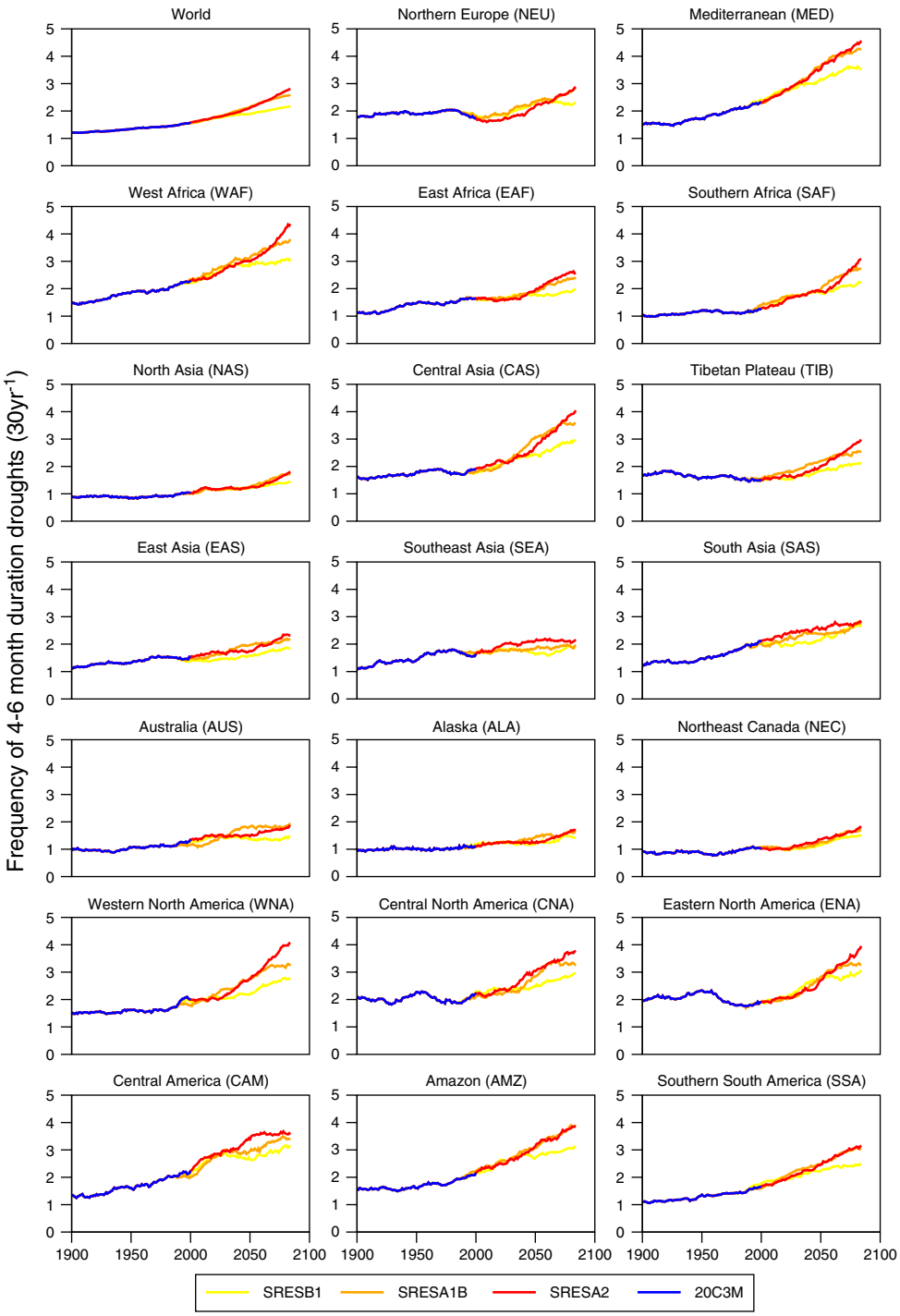

Fig. 5 Regional time series of multi-model ensemble mean of frequency of short-term droughts ($D_{4–6}$, $q_0(\theta)$ = 10.0%) for the twenty-first century for the SRESB1, SRESA1B and SRESA2 scenarios. The values are calculated over a 30-year moving window and then averaged over each region

in the winter (and throughout the rest of the year). Rain falling on the existing snow pack will also increase the rate of melting. This will in turn shift the spring melt earlier. These changes force wetter soil moisture conditions in the winter and spring, although this is offset somewhat by increased evapotranspiration due to higher temperatures. During the summer, soil moisture is reduced, despite increased precipitation, because of earlier spring melt that is compounded by evapotranspiration increases as a result of increased temperatures. The frequency of soil moisture deficits therefore increases disproportionately in the summer time compared to the wintertime.

4 Detectability of changes in drought

The detection of statistically significant changes in drought is dependent upon, among other factors, the strength of the

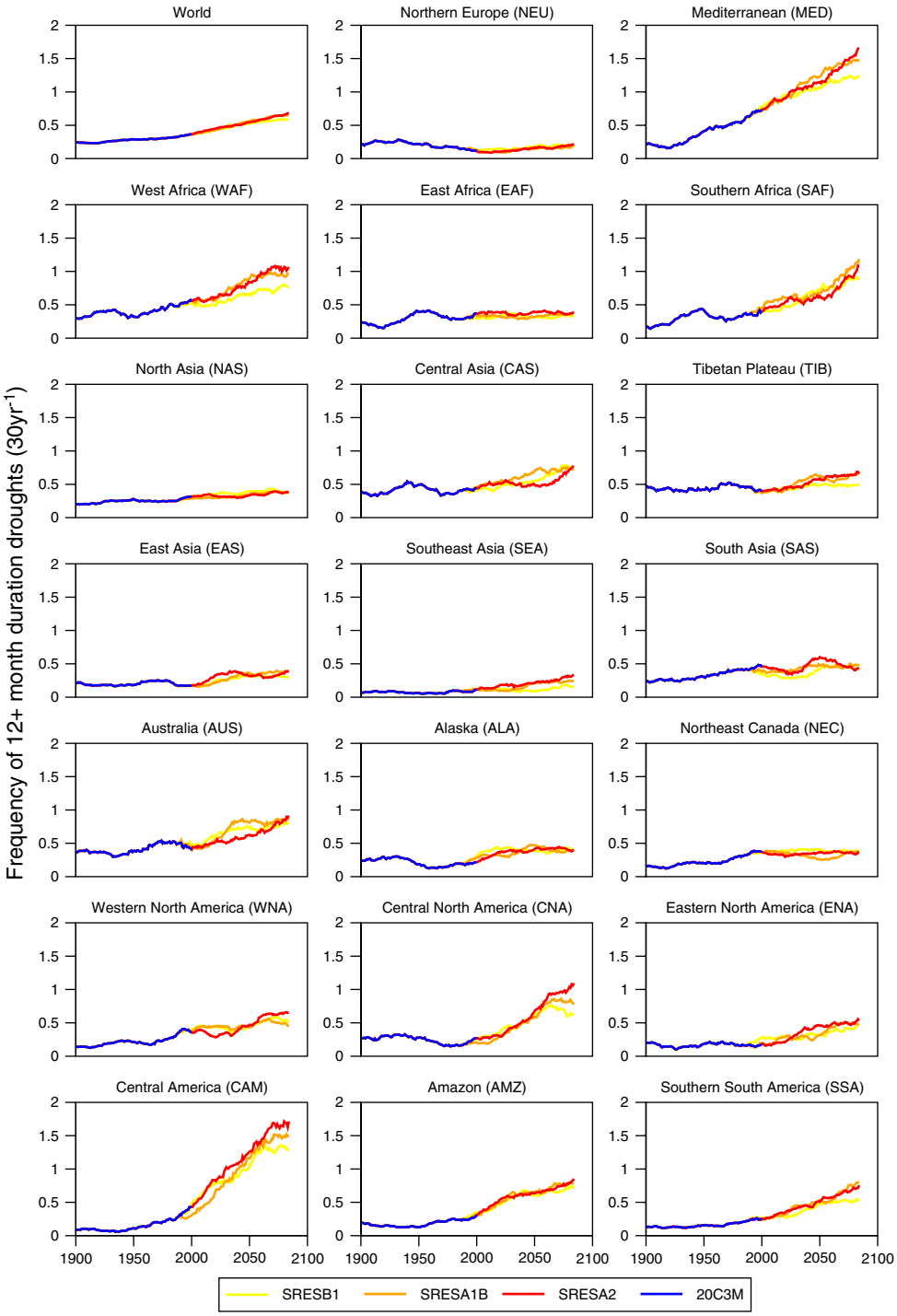

Fig. 6 As Fig. 5 but for long-term (D_{12+}) drought frequency

change (signal) against the background of natural variability (noise). As these factors vary, a change will be detected earlier or later, and the time of detection can be used to quantify detectability (e.g., Ziegler et al. 2003). The above analysis shows that statistically significant changes are predicted to occur in many regions by the end of this century, in particular the MED, SAF, CNA and CAM regions. However, these changes may actually have become significant at earlier times and there may be other regions where changes become significant or detectable at later time periods (if simulation data are available).

4.1 Examples of regional detectability

Figure 13 shows some examples of the detectability of drought occurrence for the A2 scenario for the WORLD and five regions (MED, CNA, SAF, AMZ and SAS). These

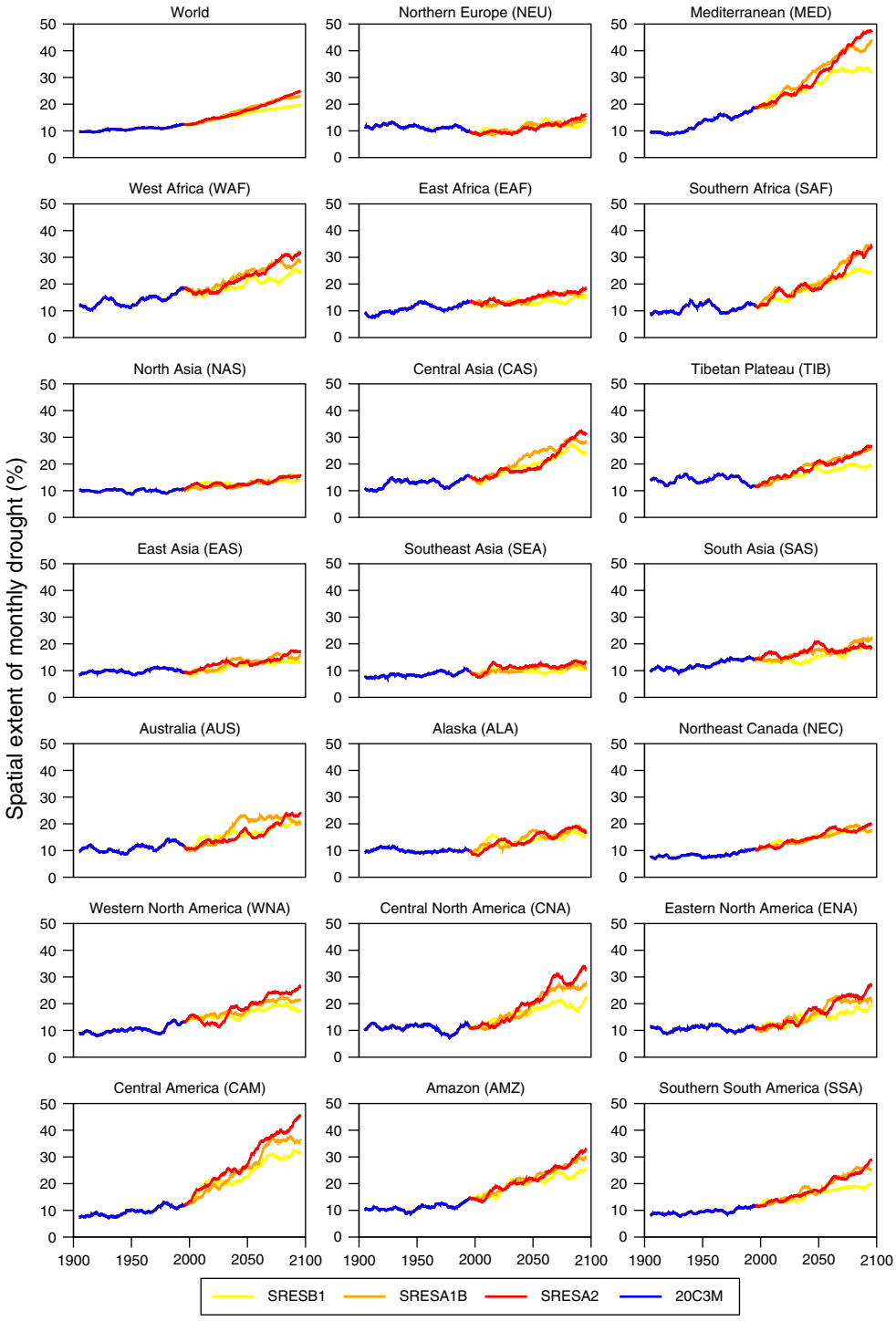

Fig. 7 As Fig. 5 but for the spatial extent of monthly drought, $q_0(\theta) = 10\%$

regions were chosen as they represent a variety of increasing drought responses (some regions, such as NEU and NAS, show no statistically significant changes). As the mean change in drought occurrence increases over time, because of, for example, decreasing precipitation, the statistical significance of the change generally also increases. Whether the changes in drought occurrence are statistically significant is dependent on the region, drought characteristic and scenario, although we only show results here for A2 (results for all scenarios are shown in Sect. 4.2). The variance (or spread) among models is also a factor. For some regions (e.g., MED) the changes are detectable by mid-twenty-first century. In others, such as WORLD, changes at the same confidence level vary by several decades between drought characteristics. Elsewhere, changes can flip between being detectable or not

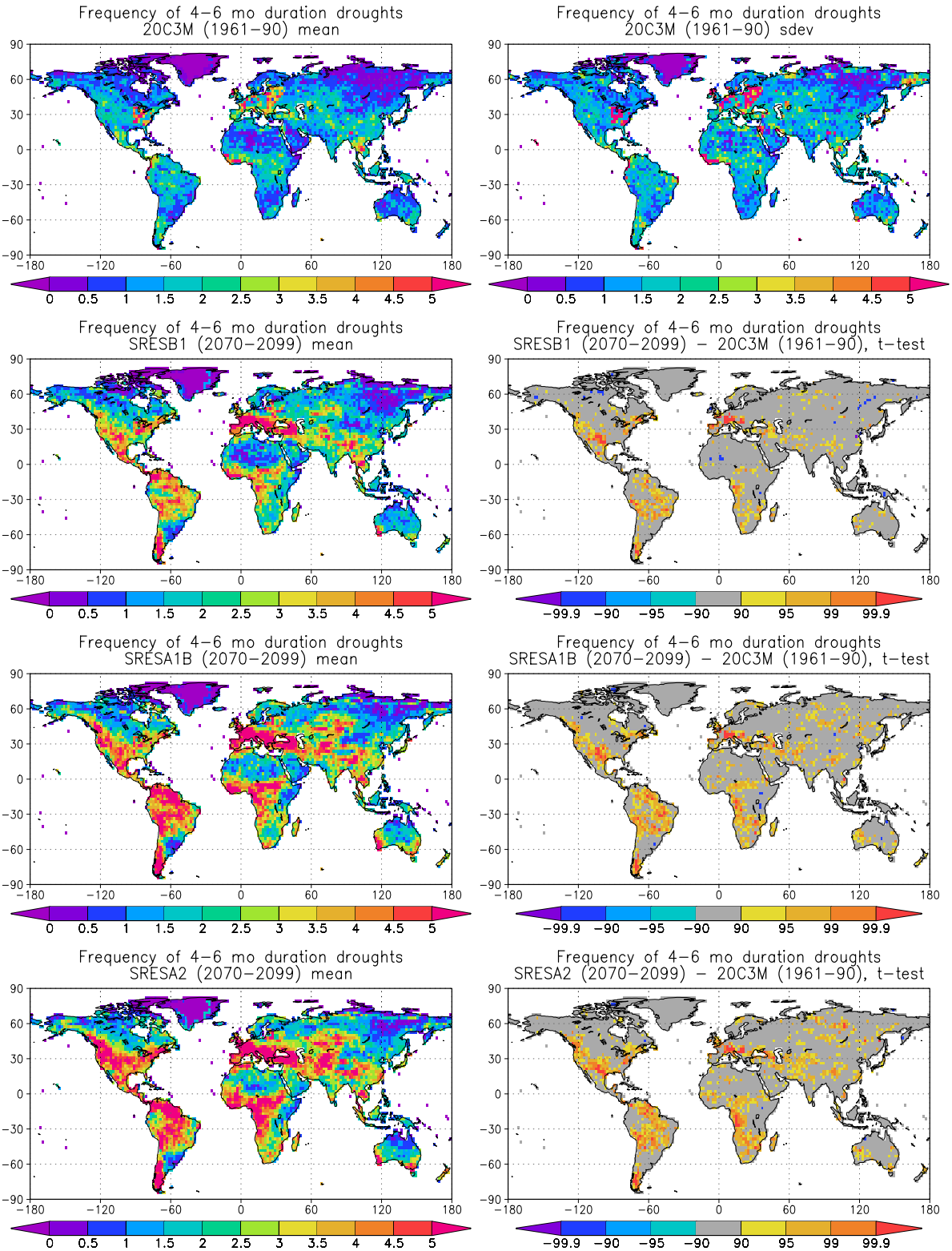

Fig. 8 Multimodel ensemble mean of frequency of D_{4-6} droughts in the 20C3M (1961–1990) simulation and for 2070–2099 in the SRESB1, SRESA1B and SRESA2 future climate scenarios. Also shown are the standard deviation of the 20C3M (1961–1990) multi-model ensemble and the statistical significance of the difference in ensemble means between the 20C3M simulation and the future climate predictions. Statistically significant changes were estimated by calculating *t* test statistics under the null hypothesis that the mean of distribution of 20C3M period drought frequency equals the mean of distribution for the future climate period. Results are shown for significance levels of 90.0, 95.0, 99.0 and 99.9% with negative values indicating a decrease in the frequency of drought

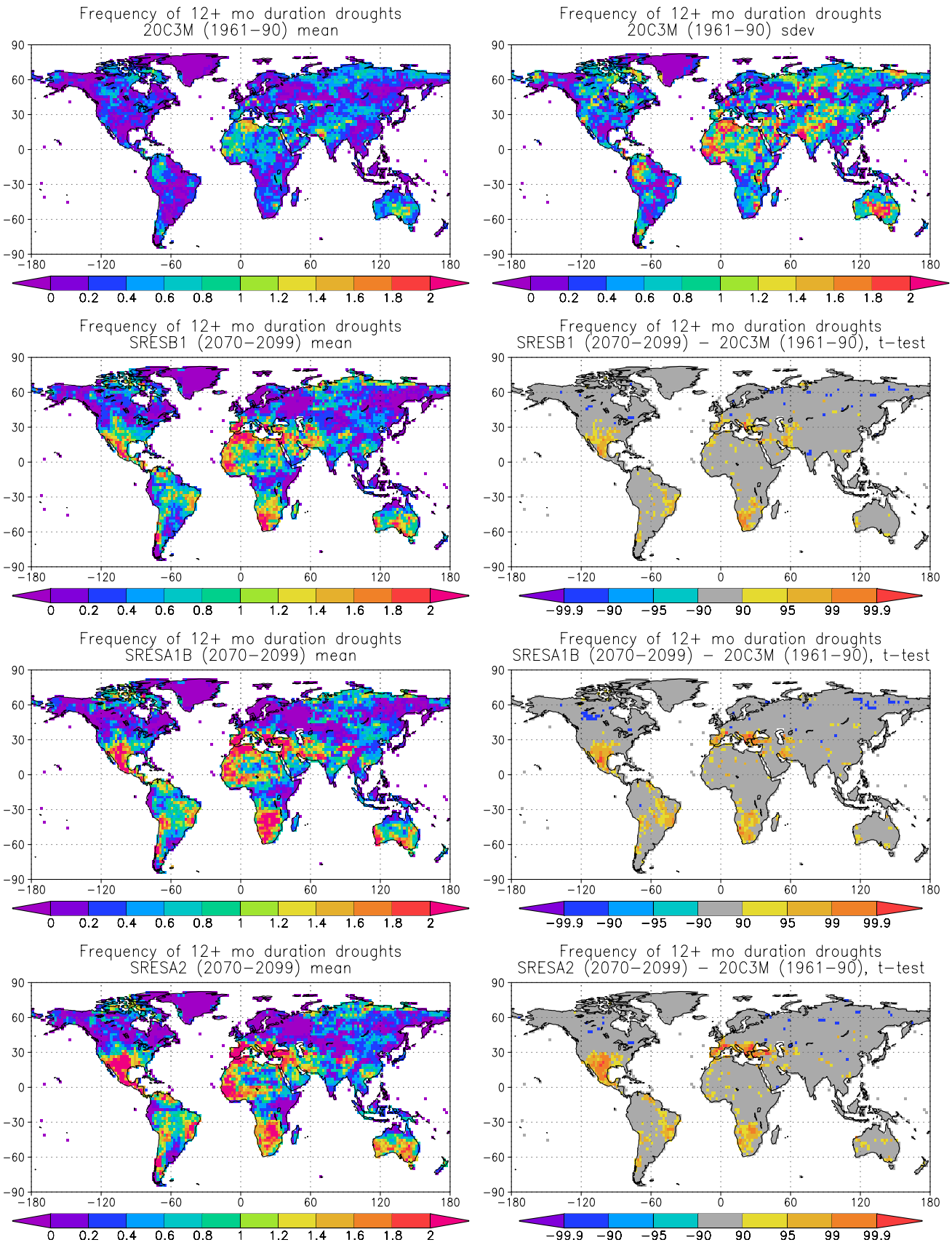

Fig. 9 As for Fig. 8, but for frequency of D_{12+} droughts

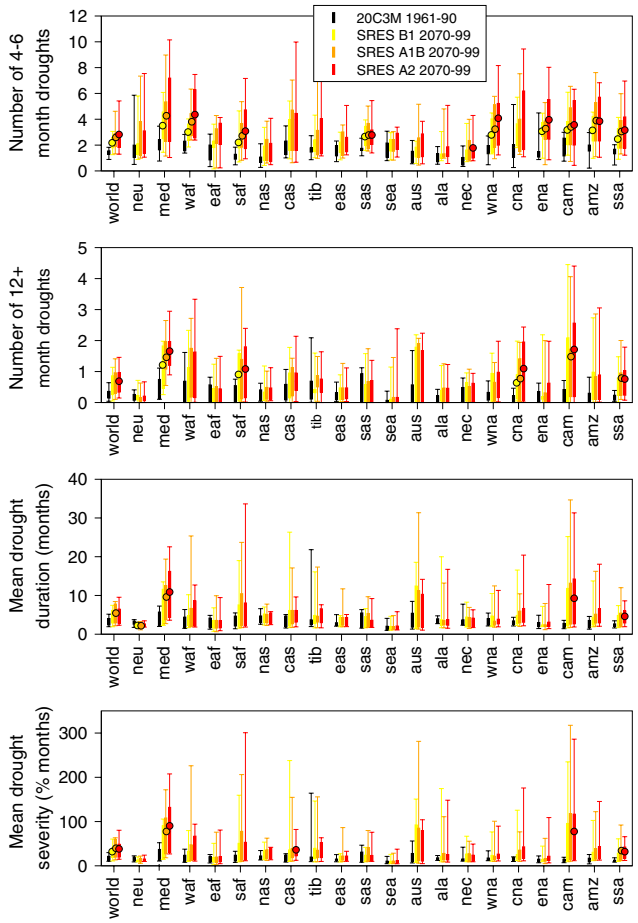

Fig. 10 Regionally averaged drought statistics for 1961–1990 (20C3M) and three future climate scenarios for 2070–2099 (SRES B1, SRES A1B, SRES A2). Drought statistics are frequency of 4–6-month duration droughts, frequency of 12+-month duration droughts, mean drought duration and mean drought severity. *Box and whispers* represent the inter quartile range and maximum and minimum values of the set of models. The mean model value is shown as *colored circles* if the change is statistically significant at the 95% level relative to 1961–1990 from the 20C3M simulation

(e.g., SAF for $D_{4–6}$ frequency) or between two levels of significance (e.g., SAS for $D_{4–6}$ frequency), which has implications for decision making based on discrete thresholds. In general, $D_{4–6}$ frequency is more detectable than D_{12+} frequency, although the CNA region shows the opposite behaviour and in the AMZ region only changes in $D_{4–6}$ frequency are detectable. Changes in $D_{4–6}$ droughts in the SAS region become detectable relatively early (around 2020) despite their small magnitude.

4.2 Detectability under different scenarios

Table 4 summarizes the detectability of changes in regional drought for the three future climate scenarios. Detectability is quantified as the mid-year of the 30-year period in which the mean change in the regional average drought characteristic first becomes statistically significant (at the 0.05 level), although in reality we would not be able to make an assessment until the end of the period once observations had been made. An earlier year of detection represents higher detectability in the predicted changes. Table 4 indicates that changes in $D_{4–6}$ frequency and drought extent are the most detectable drought characteristics. D_{12+} changes are undetectable in most regions. Changes in the MED, CAM and SSA regions are detectable for all drought characteristics and scenarios (shown previously in the end of century summary, Fig. 10) and in the WORLD and SAF regions for at least one scenario. For some regions (e.g., NEU, EAF, SEA), the changes are undetectable within the simulation period. Calculations with data from lower emission scenarios, such as B1, tend to increase the time to detection as the magnitude of the changes are lower (although variance may decrease if models show more consensus and tend to increase detectability). Detectability under higher emission scenarios is increased (detection time decreases) because the magnitude of change increases (increased signal to noise ratio), although this is complicated by the possibility that the uncertainty in future changes under higher greenhouse gas concentrations may increase the spread in model projections.

4.3 Detectability as a function of risk

The time of detection is also inherently controlled by the level of risk that one is willing to take in making the determination. The estimates in Sects. 3.3 and 4.2 are made using a conservative, low-risk probability ($\alpha = 0.05$) of making an error in detection. This low risk value could be representative of a conservative attitude to global warming in which more time is needed for detection before taking steps toward mitigating the impacts of global warming; higher risk values imply less time is required for detection. Figure 14 shows the sensitivity of detection times to the test significance. As we instil more confidence in the detection process and α decreases, our willingness to falsely detect a change when none is occurring decreases. Therefore the size of the change has to be larger for us to be confident that it is statistically different from background variability, which generally implies that we have to wait longer to detect the change and thus detectability decreases. At $\alpha = 0.05$ the detection times for changes in drought characteristics vary widely depending on the region and variable, and changes for some variables are essentially undetectable (e.g., NAS for all variables). Detection times for lower confidence levels are earlier, as expected, although often not substantially

Table 3 Regionally averaged, multi-model mean values of short- ($D_{4–6}$) and long (D_{12+}) term drought frequencies and spatial extent of drought (A), for the PICNTRL (PIC), 20C3M (1961–1990) (20C) and SRES B1, A1B, A2 (2070–2099) scenarios

	$D_{4–6}$					D_{12+}					A				
	PIC	20C	B1	A1B	A2	PIC	20C	B1	A1B	A2	PIC	20C	B1	A1B	A2
WORLD	1.1	1.4	**2.2**	**2.6**	**2.8**	0.2	0.3	0.6	0.7	**0.7**	9.2	11.2	**18.9**	**22.3**	**23.0**
NEU	1.4	2.0	2.3	2.9	2.9	0.1	0.2	0.2	0.2	0.2	9.2	11.1	12.3	13.3	14.1
MED	1.2	2.1	**3.5**	**4.3**	4.6	0.2	0.5	**1.2**	**1.5**	**1.7**	8.7	15.7	**32.7**	**41.4**	**44.7**
WAF	1.3	2.0	**3.0**	**3.8**	**4.4**	0.2	0.5	0.8	1.0	1.1	9.9	15.1	**23.0**	**27.9**	**30.2**
EAF	1.2	1.5	2.0	2.4	2.6	0.2	0.3	0.3	0.4	0.4	9.7	11.2	14.5	16.9	17.1
SAF	0.9	1.1	**2.2**	**2.7**	**3.1**	0.2	0.3	**0.9**	1.2	**1.1**	9.4	10.3	**24.3**	**31.7**	**30.7**
NAS	1.0	0.9	1.5	1.7	1.8	0.2	0.2	0.4	0.4	0.4	9.8	9.9	**13.6**	**15.0**	**14.9**
CAS	1.4	1.8	2.9	3.6	4.0	0.2	0.4	0.7	0.7	0.8	9.9	12.8	**25.0**	**27.9**	**29.2**
TIB	1.5	1.7	2.1	2.6	3.0	0.2	0.5	0.5	0.7	0.7	10.0	14.8	19.4	24.1	24.4
EAS	1.3	1.5	1.8	2.2	2.3	0.2	0.2	0.3	0.4	0.4	9.3	10.5	13.1	**15.5**	**15.7**
SAS	1.3	1.7	**2.7**	**2.8**	**2.8**	0.2	0.4	0.5	0.5	0.4	9.4	14.0	17.9	20.4	18.5
SEA	1.2	1.7	1.9	2.0	2.2	0.1	0.1	0.2	0.2	0.3	7.2	9.0	10.4	11.6	12.6
AUS	1.0	1.2	1.5	1.9	1.8	0.3	0.5	0.8	0.9	0.9	9.3	12.2	20.2	22.1	22.4
ALA	1.1	1.0	1.4	1.6	1.7	0.1	0.1	0.4	0.4	0.4	9.6	9.8	15.5	17.4	17.7
NEC	1.0	0.9	1.5	1.7	**1.8**	0.1	0.3	0.4	0.4	0.4	8.8	8.8	**17.3**	**18.3**	**18.2**
WNA	1.5	1.6	**2.8**	**3.2**	**4.1**	0.2	0.2	0.5	0.4	0.7	9.9	10.8	**18.8**	**21.3**	**24.8**
CNA	1.6	2.0	3.0	3.2	3.8	0.2	0.2	**0.6**	**0.8**	**1.1**	9.9	9.7	**20.3**	**26.3**	**30.5**
ENA	1.5	1.8	**3.1**	**3.3**	**4.0**	0.1	0.2	0.5	0.5	0.5	8.9	10.4	**18.2**	21.1	24.1
CAM	1.3	1.9	**3.2**	**3.4**	**3.7**	0.1	0.2	1.3	**1.5**	**1.7**	8.5	10.8	**30.6**	**36.0**	**41.1**
AMZ	1.4	1.7	**3.1**	**3.9**	**3.8**	0.2	0.2	0.7	0.8	0.9	9.7	11.8	**23.8**	**28.0**	**29.0**
SSA	1.3	1.4	**2.5**	**3.1**	**3.2**	0.2	0.2	0.5	**0.8**	**0.8**	9.5	10.1	**19.0**	**24.8**	**24.9**

Future values in bold are statistically significant, relative to 1961–1990 of the 20C3M simulation, at the 0.05 level with $df = 14$

different from the 95% values. However, above the 99% level, the changes generally become undetectable within the simulation period. For example, detection times for changes in D_{12+} frequency over CNA increase from about 2050 at 95% and below, to undetectable for 99% and above.

4.4 Detectability relative to natural variability

Detection of change is dependent on the background noise used to quantify the variability of the system. The results shown so far are relative to the model twentieth century simulations, which represent contemporary climate and thus encompass observed climate variability. This allows us to perceive future changes relative to the contemporary occurrence of drought of which we have first hand experience. Nevertheless, it is also of interest to know the detectability of drought changes relative to a "pristine" climate without elevated greenhouse gases, and so estimate the anthropogenic influence on drought occurrence. This was done by calculating the detectability relative to the PICNTRL simulations, and therefore assuming that these are our best estimate of natural variability. Variability in these simulations results from a number of sources including variability in solar output and internal variability of the coupled atmosphere-ocean-land system. Figure 15 gives the detection times when using either the PICNTRL or the 20C3M (1961–1990) data to estimate the background variability. Detectability generally increases when using the PICNTRL data as would be expected, because drought frequency is, in general, relatively lower in the PICNTRL compared to the 20C3M simulations (as shown in the regional statistics in Table 3). It should be noted though that decadal variability within the twentieth century means that for some regions 1961–1990 is a wet period and the changes become detectable earlier than when using the PICNTRL data.

4.5 Multi-model ensemble versus single model detectability

Given the uncertainty in future climate projections by a single model, this study is based on a multi-model ensemble. This enables us to capture the uncertainty in the representation of climate processes. However we have chosen to use a single model simulation as representative of each particular model despite the variability among same model simulations that differ only by their initial conditions. To assess how detectability differs when using the predicted climate of a single model we calculated the year

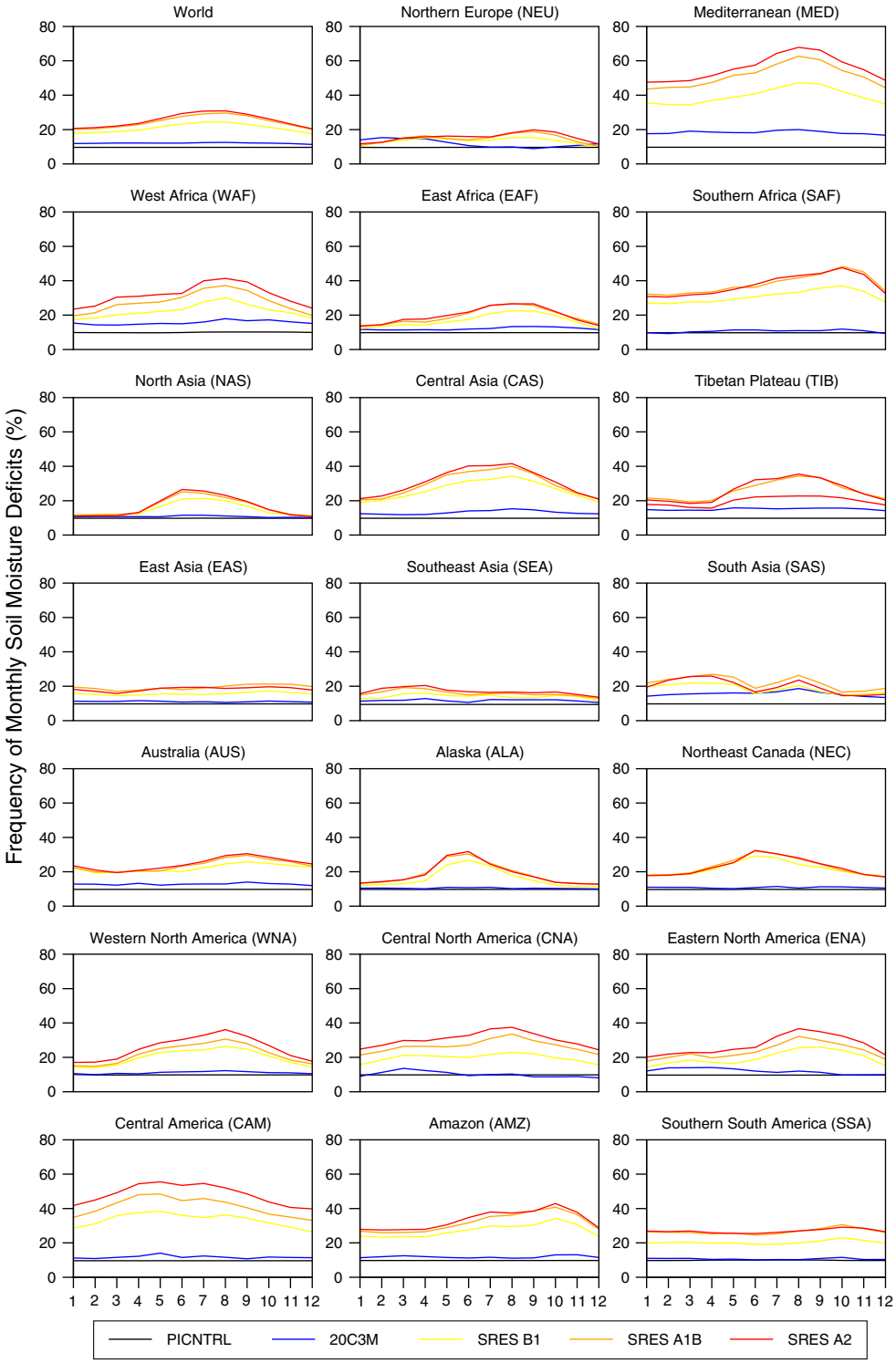

Fig. 11 Multi-model regional average of frequency of monthly soil moisture deficits for the PICNTRL, 20C3M, SRES B1, A1B and A2 scenarios, relative to the tenth percentile of the PICNTRL simulations. For each model, the number of months with soil moisture deficits below the tenth percentile soil moisture value of the PICNTRL simulation are summed and averaged across all models and the region and converted to a percentage. The values are calculated separately for each month. The PICNTRL data are by definition equal to 10% for all months. The 20C3M data are calculated for 1961–1990. The future climate SRES scenarios are calculated for 2070–2099

to detection for each of the five available ensemble members for the GISS-ER model for the A2 scenario (Fig. 16). This model was chosen because of the availability of a relatively large number of ensemble members and it is assumed that similar results would be obtained when using other models if multiple members were available. The results show reasonable agreement (within 25 years) for WAF, SAF and parts of the Americas but large differences in detectability elsewhere (e.g., the NAS and SAS regions). In general, the single model changes are detectable at earlier times. Examination of the regional time series of the single and multi-model ensembles (not shown) indicates that the

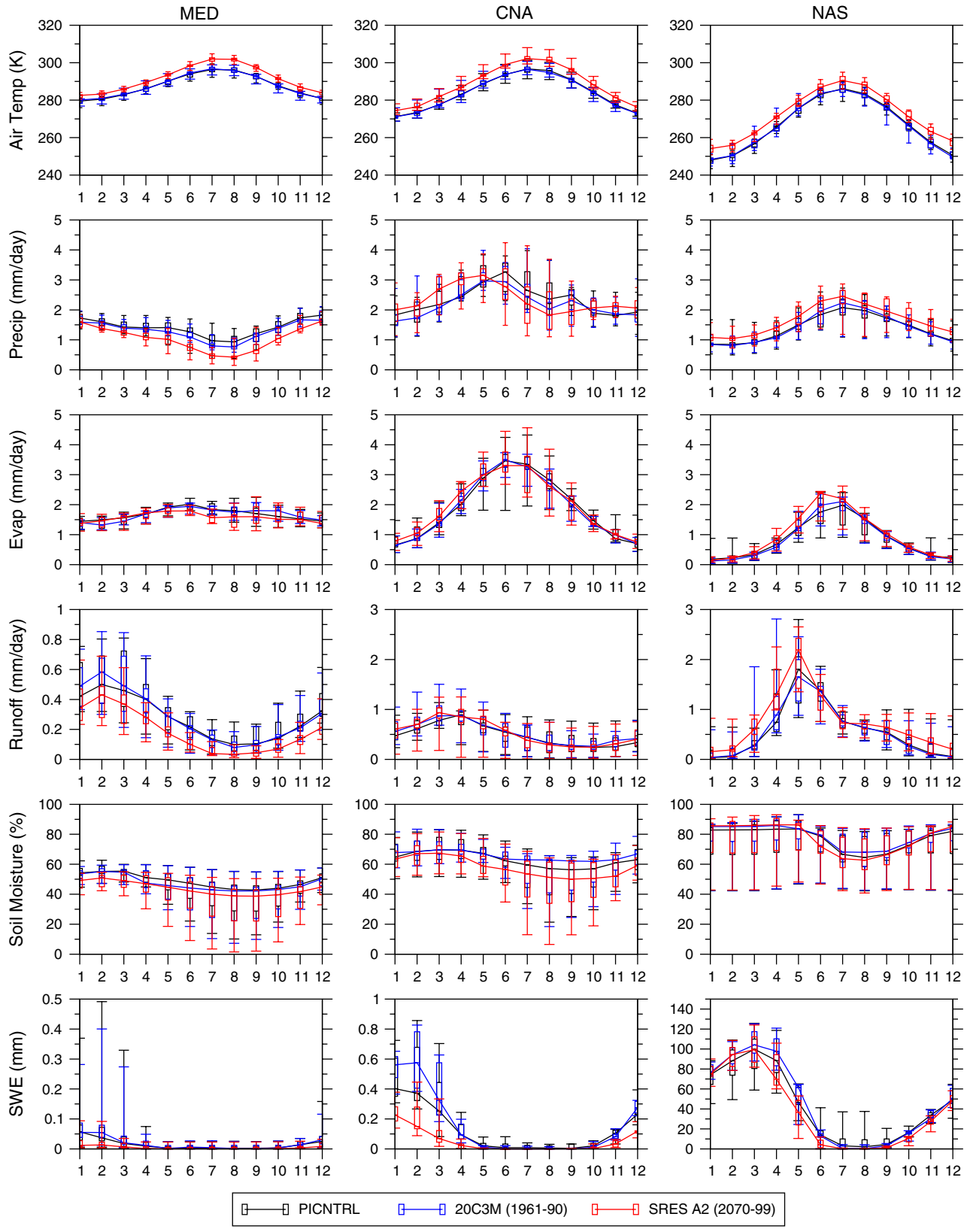

Fig. 12 Mean seasonal cycle of air temperature and the main components of the terrestrial hydrological cycle for the MED, CNA and NAS regions for the PICNTRL, 20C3M (1961–1990) and SRES A2 (2070–2099) scenarios. The *boxes and whispers* represent the inter-quartile range and range, respectively across the models

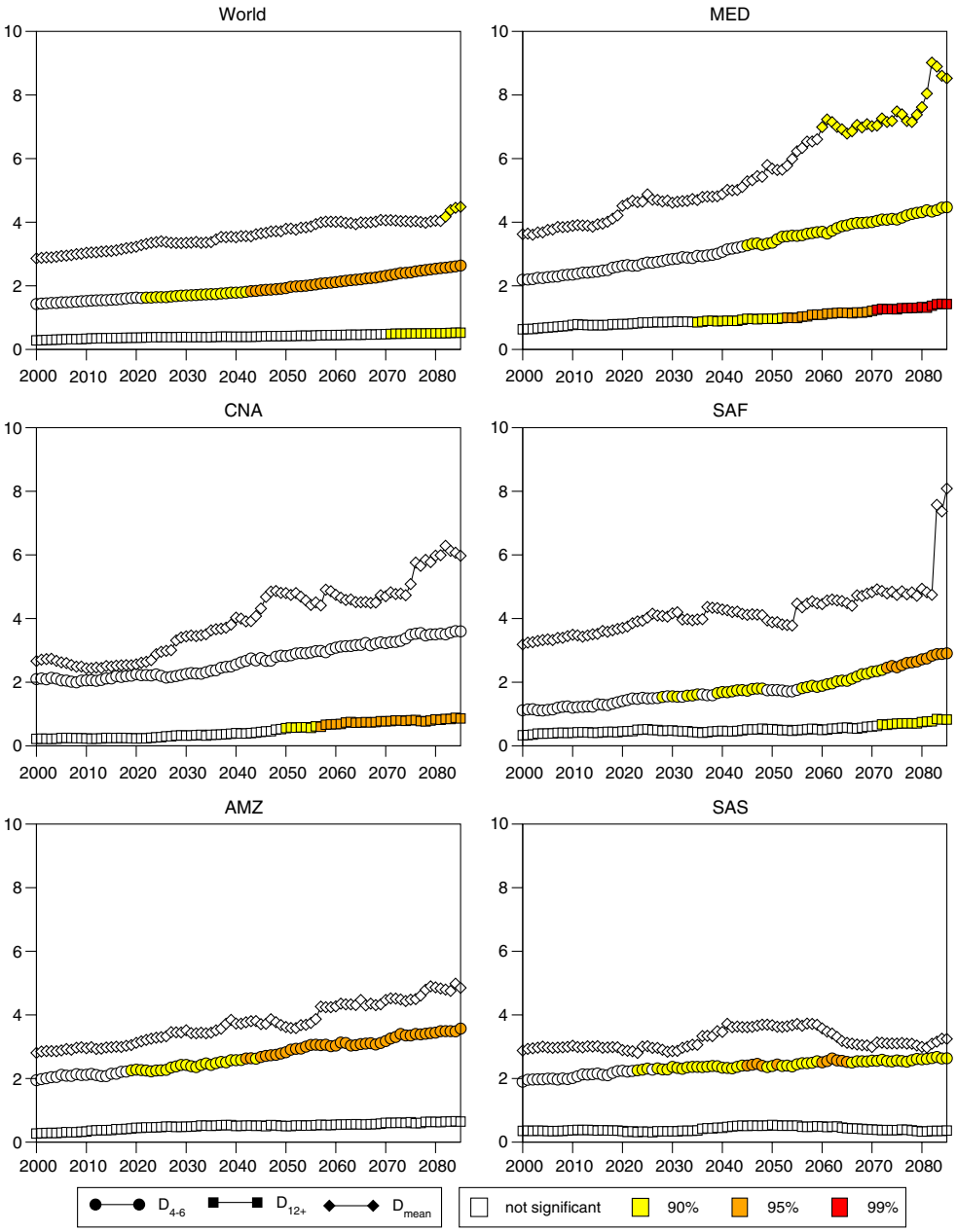

Fig. 13 Detectability of changes in SRESA2 drought occurrence for the world and five selected regions. The frequency of $D_{4–6}$ and D_{12+} droughts, and the mean drought duration D_{mean} in a 30-year moving window centred on the year is averaged over each region. The colours indicate statistical significance of the changes in drought occurrence relative to the climate model control period values at 90.0, 95.0 and 99.0% confidence levels

ensemble means are comparable in many regions and it is the larger inter-model variability relative to the single model intra-ensemble variability that gives rise to earlier detection times. For regions where single model changes are less detectable (e.g., ALA and ENA), this is generally because the changes are relatively small. For the WORLD the single model year of detection is 2026 and the multi-model values is 2000. Assuming that a multi-model ensemble gives a better estimate of the magnitude and detectability of future changes in drought occurrence (as is seen in multi-model comparisons with observations, e.g., Guo and Dirmeyer 2006), the implication is that a single model estimate may be considerably biased in some regions.

4.6 Comparison with detection times of primary climate variables

Climate change is usually described in terms of primary climate variables, such as global mean temperature and precipitation. Current estimates indicate that recent trends in temperature are statistically unusual compared with the historic (Jones and Moberg 2003) and paleoclimatic records (Osborn and Briffa 2006). For precipitation, observations are generally less extensive in time and space and are plagued by errors due to, among other factors, measurement error (e.g., wind induced under-catch), orographic effects, temporal inconsistencies, and spatial sampling errors, especially in data sparse regions

Table 4 Year of detection of statistically significant changes in drought frequency between the 20C3M (1961–1990) and the B1, A1B and A2 future scenarios from the multi-model ensemble

	D_{4-6}			D_{12+}			A		
	B1	*A1B*	*A2*	*B1*	*A1B*	*A2*	*B1*	*A1B*	*A2*
WORLD	2034	2024	2026	–	–	2079	2008	2013	2009
NEU	–	–	–	–	–	–	–	–	–
MED	2048	2046	2049	2058	2033	2038	2005	2009	2018
WAF	2024	2023	2027	–	–	–	2078	2041	2055
EAF	–	–	–	–	–	–	–	–	–
SAF	2025	2037	2040	2073	–	2074	2016	2002	2011
NAS	–	–	–	–	–	–	2064	2068	2064
CAS	–	2071	2070	–	–	–	2073	2060	2072
TIB	–	–	–	–	–	–	–	–	–
EAS	–	–	–	–	–	–	–	2081	2069
SAS	2055	2036	2025	–	–	–	–	–	–
SEA	–	–	–	–	–	–	–	–	–
AUS	–	–	–	–	–	–	–	–	–
ALA	–	–	–	–	–	–	2022	2036	–
NEC	2071	2067	2052	–	–	–	2058	2056	2048
WNA	2073	2048	2052	–	–	–	2059	2042	2040
CNA	–	–	–	2049	2053	2051	2046	2043	2035
ENA	2084	2069	2073	–	–	–	2082	2058	2079
CAM	2029	2060	2020	2056	2062	2045	2012	2024	2008
AMZ	2020	2024	2027	–	–	–	2021	2019	2027
SSA	2028	2017	2025	2058	2058	2046	2018	2012	2012

Dash symbols indicate that the change is undetectable within the simulation period. Statistical significance is calculated using the Students *t* test for a significance level of 0.05. Drought frequencies are calculated over 30-year periods and the year of detection is the middle of such a period

(Hulme and New 1997). Table 5 shows the year of detection for statistically significant changes in annual and seasonal values of surface air temperature and the main components of the terrestrial water balance for the MED region under the A2 scenario. We also repeat the detection values for drought. Air temperature changes are detectable within the first half of the twenty-first century at all time scales. Changes in precipitation (except for DJF) are also detectable but at later times, as is runoff but only for JJA and SON. For evaporation and soil moisture, changes are undetectable within the twenty-first century. The MED region was chosen as it shows some of the largest increases in drought and corresponding detectable changes in other variables. Few other regions show detectable changes, and changes at global scales are only detectable for air temperature, which is consistent with observed trends in relation to estimates of natural variability (Hansen et al. 2006; Osborn and Briffa 2006). In fact, changes in air temperature are detectable for all regions and time scales between 2003 and 2077. Changes in snow as represented by snow water equivalent (SWE) are only detectable in mid-latitudes of North America (WNA, CAN, ENA) and Asia (CAS, EAS) where variability in snow cover is higher than more northerly regions and thus likely to experience detectable changes earlier.

5 Discussion and conclusions

We have analyzed soil moisture data for three future climate scenarios from eight AOGCMs that participated in the IPCC AR4. The models show decreases in soil moisture at global scales for the future scenarios with a corresponding doubling of the spatial extent of severe soil moisture deficits and frequency of short-term (D_{4-6}) droughts from the mid-twentieth century to the end of the twenty-first. Long-term (D_{12+}) droughts become three times more common. Regionally, the MED, WAF, CAS and CAM regions show large increases, most notably for D_{12+} frequencies as do mid-latitude North American regions (WNA, CNA, ENA) but with larger variation between scenarios. Changes elsewhere are generally increasing but relatively small. Changes under the B1 scenario are the least and the A1B and A2 results are similar. We tested the statistical significance of changes at the end of the twenty-first century relative to contemporary climate as represented by the twentieth century simulations and found significant increases in D_{4-6} drought frequency globally and in most regions. Significant changes in D_{12+} frequency are less spatially extensive with increases for the MED, WAF, SAF, CAS, CAM and SSA regions for all scenarios and for TIB, CAN and AMZ for the higher emission scenarios only. Statistically significant decreases in D_{12+} frequency exist but are restricted to small areas of high latitudes.

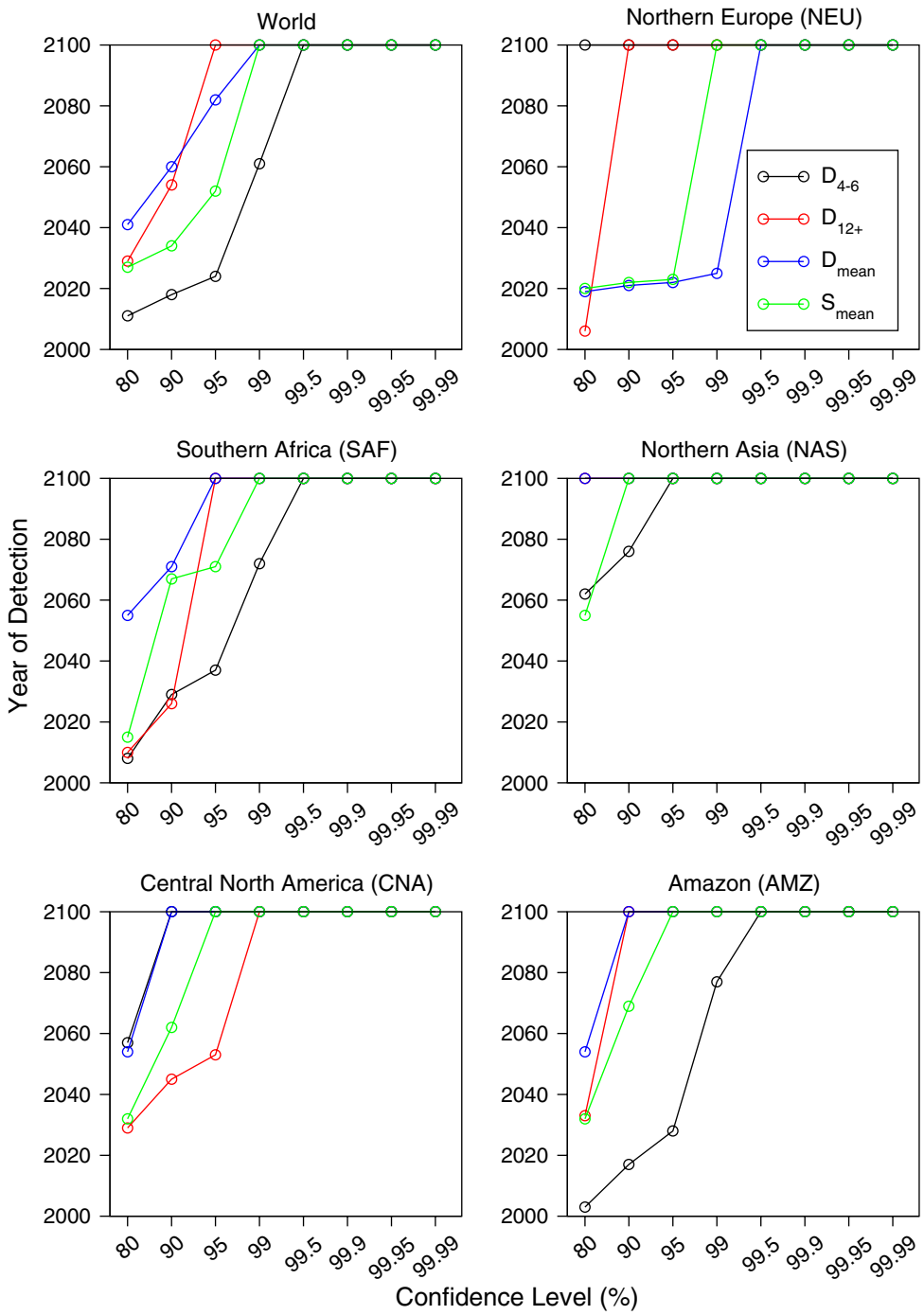

Fig. 14 Detectability as a function of statistical significance for the world and selected regions for the SRES A1B scenario. The year of detection is calculated as the mid-year of the 30-year period in which the model mean change in the drought variable is statistically different at the given significance level relative to the 20C3M (1961–1990) simulation. Detection years equal to 2100 indicate that the change is not detectable within the period of the simulation

A number of other studies have analyzed the current IPCC and other climate model simulations in terms of changes in soil moisture and drought at large scales and the results presented here are generally consistent with these. Although these studies were based on either different models (Gregory et al. 1997) and/or versions (Wetherald and Manabe 2002) or different sets of the IPCC AR4 models (Wang 2005; Burke et al. 2006) and use different metrics for defining changes in soil moisture or droughts, there is general consensus that global drying of soil moisture will occur. Wetherald and Manabe's (2002) analysis of an earlier version of the GFDL coupled model showed annual reduction in soil moisture and large reduction in summertime soil moisture in some semi-arid regions including southern North America and the Mediterranean. This is consistent with our study in terms of soil moisture (see Fig. 12 for the MED and CNA regions) and reflected in the particularly large increases in drought occurrence for the MED, CNA and CAM regions (Sect. 3.4). They also noted summer time reductions in soil

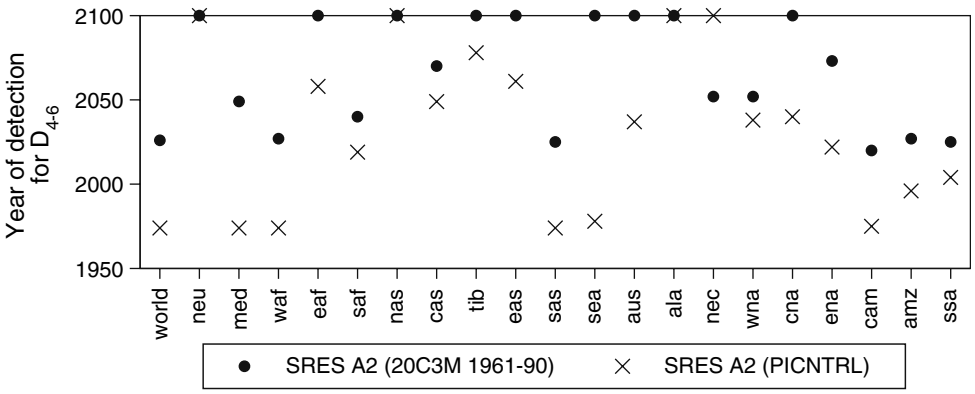

Fig. 15 Comparison of detection times for different estimates of natural variability. Detection times are when regional average changes in drought characteristics for the SRES A2 scenario become statistically different at the 0.05 level from natural variability estimated from either the PICTNRL scenario or the 20C3M scenario (1961–1990)

moisture in mid-continental middle to higher latitudes but increases in winter, which we see, for example, in the NAS region (Fig. 12).

The study of Wang (2005) has considerable overlap with this study in terms of the data used, although we use fewer models but more scenarios (Wang analyzed data from 15 models for the SRES A1B scenario) and we analyze the occurrence of drought as opposed to changes solely in the soil moisture mean. Wang found significant variation in the global pattern of changes in soil moisture, despite the direction of changes in precipitation being quite consistent across models, perhaps indicating the complexity of the soil moisture response and/or the variation across models in how they simulate surface fluxes that has been extensively noted in off-line land surface model comparisons (Wood et al. 1998; Mitchell et al. 2004; Guo and Dirmeyer 2006). This may also be a result of differences in the sub-monthly statistics, for example, the simulated storm frequencies and intensities. Only in some regions of northern mid- and high-latitudes did Wang find consistency in predicting summer dryness and winter wetness (again consistent with this study and the study of Wetherald and Manabe 2002). Elsewhere, the general consensus is for drier soils. Regions where the models were unanimous in predicting drying include southwest North America, Central America, the Mediterranean, South Africa, and Australia. This is reflected in our results that find statistically significant changes in drought occurrence in these regions (with the exception of Australia, which for our analysis showed large mean changes but with high uncertainty across models).

In terms of changes in drought specifically, Gregory et al. (1997) and Burke et al. (2006) analyzed earlier and current versions of the Hadley climate model. Despite looking at different metrics to quantify drought (Gregory et al. (1997) looked at changes in the frequency of low summer precipitation, length of dry spells and frequency of dry soils; Burke et al. (2006) looked at the PDSI as driven by climate model predicted precipitation and temperature) and different scenarios (a 1% year^{-1} increasing CO_2 concentration and the SRES A2 scenario, respectively) they found substantial drying at global scales and similar changes to this study in most regions. In both cases, a single model and single future climate scenario were considered. Crucially, both studies note that these results need to be corroborated by other climate models. The analysis of detectability from a single model (Sect. 4.5) shows how different the result can be when using one model, although the sign of changes is likely to be the same even under different scenarios. This is reflected in multi-model analyzes of soil moisture from off-line modeling, where individual models are generally capable of mimicking observed anomalies and trends (Guo and Dirmeyer 2006), but importantly, multi-model means do better at replicating

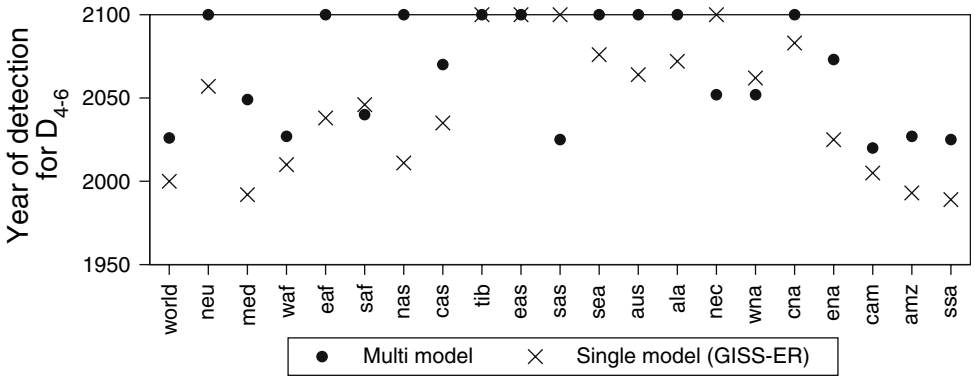

Fig. 16 Comparison of detection times for statistically significant changes (0.05 level) in regionally averaged frequency of D_{4-6} droughts for the multi model ensemble and the single model (GISS-ER) ensemble means

Table 5 Year of detection of statistically significant changes in annual and seasonal mean surface air temperature and the main components of the terrestrial water cycle (precipitation (P), evapotranspiration (E), runoff (Q), and soil moisture (SM)), and three drought characteristics for the MED region under the SRES A2 scenario

	Annual/No season	DJF	MAM	JJA	SON
T	2024	2041	2058	2034	2016
P	2063	–	2075	2064	2069
Q	–	–	–	2075	2065
E	–	–	–	–	–
SM	–	–	–	–	–
D_{4-6}	2049				
D_{12+}	2038				
A	2018				

Also shown are the detection times for drought characteristics repeated from Table 4. Note that a drought may span multiple seasons

observations than almost any individual model (Guo et al. 2007).

Wetherald and Manabe (2002) and earlier papers referenced within, provide mechanisms for summer time drying in mid-latitudes that are supported by Wang (2005). We find the same mechanisms are at play here, with reductions in precipitation the primary forcing of increased drought with increased evaporation driven by higher temperatures modulating the changes. In some regions, increases in precipitation are offset by increased evaporation. At higher latitudes where snow processes have a dominant role we see evidence for redistribution of soil moisture from spring to winter forced by earlier spring melt and a likely increased rain to snow ratio during the cooler seasons. This has a knock-on effect during the summer when reduced soil moisture persistence from the spring coupled with increased evaporative demand from increased temperatures conspires to reduce soil moisture, also found by Wang (2005). Note that we have not investigated the reasons for changes in the forcings of drought themselves. Modeling studies suggest though, that large-scale change in atmospheric circulation as driven by Tropical SSTs is the dominant mechanism for changes in regional precipitation, as opposed to thermodynamic processes at local or large scales (Findell and Delworth 2005).

Although the predicted future changes in drought occurrence are essentially monotonic increasing globally and in many regions, they are generally not statistically different from natural variability for multiple decades. Detectability of change is however dependent on many factors, including the magnitude of the change, and the background noise or natural variability as estimated from the control simulations, which in turn depend on the type of drought statistic. It also depends on the chosen level of significance in the statistical testing or risk that one is willing to take in detecting the impacts of climate change. As this is generally an arbitrary choice the implication is that this can by itself introduce great uncertainty in the detection of climate change. A 95% confidence level is ubiquitous in the scientific literature, but a 90 or 99% confidence level could just as easily be used with dramatic changes in the results as seen for the example of CNA in Fig. 14.

In contrast to primary climate variables, such as global mean surface air temperature, changes in drought are predicted to become detectable only after multiple decades, if at all. This lag can be crucial with respect to implementing mitigative or adaptive measures against such changes (Pittock 1999). On the other hand, changes in annual and seasonal means of terrestrial hydrologic variables, including soil moisture, are essentially undetectable within the twenty-first century. Although related studies of future drought occurrence (e.g., Wetherald and Manabe 2002; Wang 2005) focused on changes in the mean, such as mean monthly precipitation or soil moisture, it has been noted (Gregory et al. 1997; Kharin and Zwiers 2005) that changes in the mean are accompanied by lengthening of distribution tails and larger changes in extremes, such as drought as shown here. The implication is that changes in the extremes of climate and their hydrological impacts may be more detectable than changes in mean climate, although observing and quantifying extreme events, and comparing them to model output, is much harder in practice (Hergerl et al. 2006).

Despite the robustness of the changes in drought, globally and across many regions, and for all scenarios, there are still many uncertainties in this study that arise not only from our approach but also from the simulations themselves. Firstly, we have by necessity used eight models to represent the uncertainty across models, although 24 models contributed data for one or more scenarios to the IPCC AR4. The error in doing this is difficult to quantify but our estimates are consistent with results for a larger set of models for a single scenario (Wang 2005). Secondly, the models themselves may be biased because of inadequacies in the modeled physical processes and parameterizations and because of processes that are not included in the modeling. Such biases can generally be evaluated by comparison with observed conditions and this is critical for confidence to be instilled in future projections.

Evaluation of the models' ability to replicate observed climate variability and the terrestrial water cycle has been addressed elsewhere with mixed results (e.g., Dai 2006; Frei and Gong 2005; Lau et al. 2006; Li et al. 2007; Swenson and Milly 2006). For drought specifically, we have shown that the models do reasonably well in

replicating our best estimates of twentieth century drought statistics at regional scales yet with large spread among the models and a general over-estimation of drought duration and frequency (especially for long-term drought). Note that the off-line drought values are estimates that are subject to uncertainty in themselves. However, we currently consider the VIC off-line dataset our best estimate of global drought conditions, in the most part because it has been evaluated in terms of its depiction of large-scale drought (Sheffield and Wood 2007), directly through assessment of historic drought events and indirectly through validation of the underlying hydrologic fluxes and states. Furthermore, comparison of modeled soil moisture variability from multiple off-line models indicates that inter-model differences are small (Guo and Dirmeyer 2006), which leads us to believe that comparable estimates would be obtained if a different model was used.

The reasons for the difference between the climate models and the off-line dataset are unclear at present, and a more detailed evaluation of these models in terms of their representation of drought is work in progress that will be reported elsewhere by the authors. Potential candidates for explaining some of the differences include model biases in the characteristics of precipitation, especially the frequency and intensity of individual events (Dai 2006), and the strength of land–atmosphere coupling (Dirmeyer et al. 2006), which impacts the persistence of anomalies. Climate models may actually do better at replicating atmospheric and large-scale climate variability (e.g., AchutaRao and Sperber 2006), but the uncertainty in modeled land surface processes (precipitation, soil moisture and their feedbacks in particular) coupled with the uncertainties in future climate projections is reason to incorporate as many models as possible in any assessment of future change.

Processes that have a direct impact on drought occurrence but are not present in the models include anthropogenic forcings such as irrigation, water diversion and land use and natural processes such as vegetation dynamics and wildfire. Anthropogenic processes are difficult to quantify, even historically. Estimates of current day irrigation are that 16.3% of cultivated regions are equipped for irrigation (Siebert et al. 2005) which can have a significant impact on the water cycle (Haddeland et al. 2007), although historically this may have been offset by changes in land use. The impact of vegetation dynamics, through feedbacks with climate and interactions with climate induced changes in plant phenology and species composition may have a profound impact on drought occurrence through controls on water use, with potential positive feedbacks from natural deforestation (Cox et al. 2000; Gullison et al. 2007).

Notwithstanding the uncertainties in detectability, we can make some final general observations regarding the results. The consensus among this set of the latest GCM projections of future climates is that drought frequency will increase relative to the contemporary climate but will not show statistically significant changes for several decades, indicating that the impacts of climate change will not be felt immediately at regional scales. In general, there is a greater propensity to increased warm season drought which may be especially pertinent when specific impacts are taken into consideration, such as drought effects on agriculture that are most important during the growing season. Drought is shown to increase under all scenarios, including the B1 scenario that follows a reduced greenhouse gas emission pathway through the twenty-first century relative to the present day. The implication is that drought occurrence will increase, despite future emission reductions and this will be exacerbated by the thermal inertia of the oceans (Wigley 2005; Meehl et al. 2005) and already accumulated greenhouse gases, which in turn will increase the time to stabilization of concentrations. Under high emission pathways (A1B and A2), the magnitude of the drought changes are expected to be even higher, but more worrisome is that these scenarios may already be underestimating observed changes as has been seen since the IPCC Third Assessment Report simulations (Rhamstorf et al. 2007).

Acknowledgments This work was partly supported by U.S. Department of Energy grant 983338. We acknowledge the modeling groups for making their simulations available for analysis, the Program for Climate Model Diagnosis and Intercomparison (PCMDI) for collecting and archiving the CMIP3 model output, and the WCRP's Working Group on Coupled Modeling (WGCM) for organizing the model data analysis activity. The WCRP CMIP3 multi-model dataset is supported by the Office of Science, U.S. Department of Energy. We would also like to thank the two anonymous reviewers for their thoughtful comments that helped improve this work.

References

Achuta Rao K, Sperber KR (2006) ENSO simulation in coupled ocean–atmosphere models: are the current models better? Clim Dyn. doi:10.1007/s00382-006-0119-7

Brohan P, Kennedy JJ, Haris I, Tett SFB, Jones PD (2006) Uncertainty estimates in regional and global observed temperature changes: a new dataset from 1850. J Geophys Res 111:D12106. doi: 10.1029/2005JD006548

Burke EJ, Brown SJ, Christidis N (2006) Modeling the recent evolution of global drought and projections for the twenty-first century with the hadley centre climate model. J Hydrometeorol 7:1113–1125

Christensen E, Lassen K (1991) Length of the solar cycle: an indicator of solar activity closely associated with climate. Science 254:698–700

Ciais P et al (2005) Europe-wide reduction in primary productivity caused by the heat and drought in 2003. Nature 437:529–533

Collins M, Osborn TJ, Tett SFB, Briffa KR, Schweingruber FH (2002) A comparison of the variability of a climate model with paleotemperature estimates from a network of tree-ring densities. J Clim 15:1497–1515

Cox PM, Betts RA, Jones CD, Spall SA, Totterdell IJ (2000) Acceleration of global warming due to carbon-cycle feedbacks in a coupled climate model. Nature 408:184–187

Dai A (2006) Precipitation characteristics in eighteen coupled climate models. J Clim 19:4605–4630

Dai A, Trenberth KE, Karl TR (1998) Global variations in droughts and wet spells: 1900–1995. Geophys Res Lett 25(17):3367–3370

Dirmeyer PA, Koster RD, Guo ZC (2006) Do global models properly represent the feedback between land and atmosphere? J Hydrometeorol 7:1177–1198

Easterling DR, Meehl GA, Parmesan C, Changnon SA, Karl TR, Mearns LO (2000) Climate extremes: observations, modeling, and impacts. Science 289:2068–2074

Findell KL, Delworth TL (2005) A modeling study of dynamic and thermodynamic mechanisms for summer drying in response to global warming. Geophys Res Lett 32:L16702. doi: 10.1029/2005GL023414

Frei A, Gong G (2005) Decadal to century scale trends in North American snow extent in coupled atmosphere–ocean General Circulation Models. Geophys Res Lett 32:L18502

Giorgi F (2006) Climate change hot-spots. Geophys Res Lett 33:4

Giorgi F, Bi X (2005) Updated regional precipitation and temperature changes for the 21st century from ensembles of recent AOGCM simulations. Geophys Res Lett 32(21):4

Giorgi F, Francisco R (2000) Uncertainties in regional climate change prediction: a regional analysis of ensemble simulations with the HADCM2 coupled AOGCM. Clim Dyn 16:169–182

Gregory JM, Mitchell JFB, Brady AJ (1997) Summer drought in northern midlatitudes in a time-dependent CO_2 climate experiment. J Clim 10:662–686

Gullison RE, Frumhoff PC, Canadell JG, Field CB, Nepstad DC, Hayhoe K, Avissar R, Curran LM, Friedlingstein P, Jones CD, Nobre C (2007) Tropical forests and climate policy. Science 316(5827):985. doi:10.1126/science.1136163

Guo ZC, Dirmeyer PA (2006) Evaluation of the second global soil wetness project soil moisture simulations: 1. Intermodel comparison. J Geophys Res Atmos 111(D22):14

Guo Z, Dirmeyer PA, Gao X, Zhao M (2007) Improving the quality of simulated soil moisture multi-model ensemble approach. Q J R Meteorol Soc 133:731–747. doi:10.1002/qj.48

Haddeland I, Skaugen T, Lettenmaier DP (2007) Hydrologic effects of land and water management in North America and Asia: 1700–1992. Hydrol Earth Sys Sci 11(2):1035–1045

Hansen J, Ruedy R, Glascoe J, Sato Mki (1999) GISS analysis of surface temperature change. J Geophys Res 104:30997–31022. doi: 10.1029/1999JD900835

Hansen J, Sato M, Ruedy R, Lo K, Lea DW, Medina-Elizade M (2006) Global temperature change. Proc Natl Acad Scie USA 103:14288–14293

Hasselmann K, Latif M, Hooss G, Azar C, Edenhofer O, Jaeger CC, Johannessen OM, Kemfert C, Welp M, Wokaun A (2003) The challenge of long-term climate change. Science 302:1923–1925

Hegerl GC, Karl TR, Allen M, Bindoff NL, Gillett N, Karoly D, Zhang XB, Zwiers F (2006) Climate change detection and attribution: beyond mean temperature signals. J Clim 19:5058–5077

Held IM, Soden BJ (2000) Water vapor feedback and global warming. Ann Rev Energy Environ 25:441–475

Higgins RW, Leetmaa A, Xue Y, Barnston A (2000) Dominant factors influencing the seasonal predictability of US precipitation and surface air temperature. J Clim 13:3994–4017

Hulme M, New M (1997) Dependence of large-scale precipitation climatologies on temporal and spatial sampling. J Clim 10:1099–1113

Hulme M, Barrow EM, Arnell NW, Harrison PA, Johns TC, Downing TE (1999) Relative impacts of human-induced climate change and natural climate variability. Nature 397:688–691

Hunt BG (2006) The medieval warm period, the little ice age and simulated climatic variability. Clim Dyn 27:677–694

Huntington TG (2006) Evidence for intensification of the global water cycle: review and synthesis. J Hydrol 319:83–95

IPCC (2001) Climate change 2001: the scientific basis. In: Houghton JT et al (eds) Contribution of Working Group I to the Third Assessment Report of the Intergovernmental Panel on Climate Change. Cambridge University Press, Cambridge, 944 pp

IPCC (2007) Climate change 2007: the physical science basis. In: Solomon S, Qin D, Manning M, Chen Z, Marquis M, Averyt KB, Tignor M, Miller HL (eds) Contribution of Working Group I to the fourth assessment report of the intergovernmental panel on climate change. Cambridge University Press, Cambridge, 996 pp

Jansen E, Overpeck J, Briffa KR, Duplessy J-C, Joos F, Masson-Delmotte V, Olago D, Otto-Bliesner B, Peltier WR, Rahmstorf S, Ramesh R, Raynaud D, Rind D, Solomina O, Villalba R, Zhang D (2007) Palaeoclimate. In: Solomon S, Qin D, Manning M, Chen Z, Marquis M, Averyt KB, Tignor M, Miller HL (eds) Climate change 2007: the physical science basis. Contribution of Working Group I to the fourth assessment report of the intergovernmental panel on climate change. Cambridge University Press, Cambridge

Jones PD, Moberg A (2003) Hemispheric and large-scale surface air temperature variations: an extensive revision and an update to 2001. J Clim 16:206–223

Jones PD, New M, Parker DE, Martin S, Rigor IG (1999) Surface air temperature and its variations over the last 150 years. Rev Geophys 37:173–199

King DA (2004) Climate change science:adapt, mitigate, or ignore? Science 303:176–177

Kharin VV, Zwiers FW (2005) Estimating extremes in transient climate change simulations. J Clim 18:1156–1173

Lau K-M, Shen S, Kim K-M, Wang H (2006) A multi-model study of the 20th century simulations of Sahel drought from the 1970s to 1990s. J Geophys Res 111:D0711. doi: 10.1029/2005JD006281

Li H, Robock A, Wild M (2007) Evaluation of intergovernmental panel on climate change fourth assessment soil moisture simulations for the second half of the twentieth century. J Geophys Res 112:D06106. doi: 10.1029/2006JD007455

Maurer EP, Wood AW, Adam JC, Lettenmaier DP, Nijssen B (2002) A long-term hydrologically-based data set of land surface fluxes and states for the conterminous United States. J Clim 15:3237–3251

McCabe GJ Jr, Wolock DM (1997) Climate change and the detection of trends in annual runoff. Clim Res 8:129–134

Meehl GA et al (2005) How much more global warming and sea level rise? Science 307(5716):1769–1772

Mitchell KE, 22 coauthors (2004) The multi-institution North American Land Data Assimilation System (NLDAS): Utilizing multiple GCIP products and partners in a continental distributed hydrological modeling system. J Geophys Res 109:D07S90. doi: 10.1029/2003JD003823

Nakićenović N, Davidson O, Davis G, Grübler A, Kram T, Rovere ELL, Metz B, Morita T, Pepper W, Pitcher H, Sankovski A, Shukla P, Swart R, Watson R, Dadi Z (2000) Emissions scenarios—summary for policymakers. Intergovernmental Panel on Climate Change, Geneva

NRC (2003) Understanding climate change feedbacks. Report of the Panel on Climate Change Feedbacks, National Research Council. National Academies Press, Washington, 166pp

Osborn T, Briffa KR (2006) The spatial extent of 20th-century warmth in the context of the past 1200 years. Science 311:841–844

Palmer TN, Räisänen J (2002) Quantifying the risk of extreme seasonal precipitation events in a changing climate. Nature 415:512–514

Pittock AB (1999) Climate change: the question of significance. Nature 397:657–658

Rahmstorf S, Cazenave A, Church JA, Hansen JE, Keeling RF, Parker DE, Somerville RCJ (2007) Recent climate observations compared to projections. Science 316(5825):709

Rind D, Goldberg R, Hansen J, Ruedy C, Rosenzweig C (1990) Potential evapotranspiration and the likelihood of future drought. J Geophys Res 95:9983–10004

Robock A, Mao J (1995) The volcanic signal in surface temperature observations. J Clim 8:1086–1103

Robock A, Vinnikov KY, Srinivasan G, Entin JK, Hollinger SE, Speranskaya NA, Liu SX, Namkhai A (2000) The global soil moisture data bank. Bull Am Meteorol Soc 81:1281–1299

Seneviratne SI, Luthi D, Litschi M, Schar C (2006a) Land–atmosphere coupling and climate change in Europe. Nature 443:205–209

Seneviratne SI, Koster RD, Guo ZC, Dirmeyer PA, Kowalczyk E, Lawrence D, Liu P, Lu CH, Mocko D, Oleson KW, Verseghy D (2006b) Soil moisture memory in AGCM simulations: analysis of global land–atmosphere coupling experiment (GLACE) data. J Hydrometeorol 7:1090–1112

Sheffield J, Wood EF (2007) Characteristics of global and regional drought, 1950–2000: analysis of soil moisture data from off-line simulation of the terrestrial hydrologic cycle. J Geophys Res 112:D17115. doi: 10.1029/2006JD008288

Siebert S, Döll P, Hoogeveen J, Faures J-M, Frenken K, Feick S (2005) Development and validation of the global map of irrigation areas. Hydrol Earth Syst Sci 9:535–547

Sheffield J, Goteti G, Wen F, Wood EF (2004) A simulated soil moisture based drought analysis for the United States. J Geophys Res 109:D24108. doi: 10.1029/2004JD005182

Sheffield J, Goteti G, Wood EF (2006) Development of a 50-year high-resolution global dataset of meteorological forcings for land surface modeling. J Clim 19:3088–3111

Swenson SC, Milly PCD (2006) Climate model biases in seasonality of continental water storage revealed by satellite gravimetry. Water Resour Res 42:W03201. doi: 10.1029/2005WR004628

Trenberth KE (1999) Atmospheric moisture recycling: role of advection and local evaporation. J Clim 12:1368–1381

Trenberth KE, Hurrell JW (1994) Decadal atmosphere–ocean variations in the Pacific. Clim Dyn 9:303

Wang GL (2005) Agricultural drought in a future climate: results from 15 global climate models participating in the IPCC 4th assessment. Clim Dyn 25:739–753

Wetherald RT, Manabe S (1995) The mechanisms of summer dryness induced by greenhouse warming. J Clim 8:3096–3108

Wetherald RT, Manabe S (1999) Detectability of summer dryness caused by greenhouse warming. Climatic Change 43:495–511

Wetherald RT, Manabe S (2002) Simulation of hydrologic changes associated with global warming. J Geophys Res 107(D19):4379

Wigley TML (2005) The climate change commitment. Science 307(5716):1766–1769

Wilhite DA (2000) Drought as a natural hazard: concepts and definitions. In: Wilhite DA (Ed) Drought: a global assessment. Routledge, New York, pp 3–18

Wood EF, Lettenmaier DP, Liang X, Lohmann D, Boone A, Chang S, Chen F, Dai YJ, Dickinson RE, Duan QY, Ek M, Gusev YM, Habets F, Irannejad P, Koster R, Mitchell KE, Nasonova ON, Noilhan J, Schaake J, Schlosser A, Shao YP, Shmakin AB, Verseghy D, Warrach K, Wetzel P, Xue YK, Yang ZL, Zeng QC (1998) The project for intercomparison of land-surface parameterization schemes (PILPS) phase 2(c) Red-Arkansas River basin experiment: 1. Experiment description and summary intercomparisons. Global Planet Change 19:115–135

Zheng X, Basher RE (1999) Structural time series models and trend detection in global and regional temperature series. J Clim 12:2347–2358

Ziegler AD, Sheffield J, Maurer EP, Nijssen B, Wood EF, Lettenmaier DPL (2003) Detection of intensification in global- and continental-scale hydrological cycles: temporal scale of evaluation. J Clim 16:535–547